

**NASA TECHNICAL
MEMORANDUM**



NASA TM X-3030

NASA TM X-3030

(NASA-TM-X-3030) EFFECT OF RATIO OF
WALL BOUNDARY LAYER THICKNESS TO JET
DIAMETER ON MIXING OF A NORMAL HYDROGEN
JET IN A SUPERSONIC STREAM (NASA) 45 42-P
HC \$3.25

N74-26826

Unclas

42013

CSCL 20D

H1/12



**EFFECT OF RATIO OF
WALL BOUNDARY-LAYER THICKNESS
TO JET DIAMETER ON MIXING
OF A NORMAL HYDROGEN JET
IN A SUPERSONIC STREAM**

by Charles R. McClinton
Langley Research Center
Hampton, Va. 23665



1. Report No. NASA TM X-3030	2. Government Accession No.	3. Recipient's Catalog No.	
4. Title and Subtitle EFFECT OF RATIO OF WALL BOUNDARY-LAYER THICKNESS TO JET DIAMETER ON MIXING OF A NORMAL HYDROGEN JET IN A SUPERSONIC STREAM		5. Report Date June 1974	
		6. Performing Organization Code	
7. Author(s) Charles R. McClinton		8. Performing Organization Report No. L-9455	
		10. Work Unit No. 501-04-03-03	
9. Performing Organization Name and Address NASA Langley Research Center Hampton, Va. 23665		11. Contract or Grant No.	
		13. Type of Report and Period Covered Technical Memorandum	
12. Sponsoring Agency Name and Address National Aeronautics and Space Administration Washington, D.C. 20546		14. Sponsoring Agency Code	
15. Supplementary Notes			
16. Abstract A preliminary experimental program was conducted to determine the effect of the ratio of the free-stream boundary-layer thickness to jet diameter on the secondary jet penetration and mixing rate. Tests were conducted on a flat plate in a Mach number 4.05 airflow with sonic injection of hydrogen normal to the free-stream direction from circular underexpanded injectors. The ratio of boundary-layer thickness to jet diameter ranged from 1.25 to 6.5. Previous correlations of mixing performance were modified to account for the effect of the ratio of boundary-layer thickness to jet diameter.			
17. Key Words (Suggested by Author(s)) Fuel mixing Secondary jet penetration Scramjet		18. Distribution Statement Unclassified - Unlimited	
		STAR Category 12	
19. Security Classif. (of this report) Unclassified	20. Security Classif. (of this page) Unclassified	21. No. of Pages 45	22. Price* \$3.25

EFFECT OF RATIO OF WALL BOUNDARY-LAYER THICKNESS TO
JET DIAMETER ON MIXING OF A NORMAL HYDROGEN JET
IN A SUPERSONIC STREAM

By Charles R. McClinton
Langley Research Center

SUMMARY

This report contains results from a preliminary experimental investigation conducted to study the effect of the ratio of boundary-layer thickness to jet diameter δ/D on the mixing of hydrogen injected sonically from a flat plate into a supersonic air free stream. Several values of jet diameter D and free-stream total pressure were used to vary δ/D over the range $1.25 \leq \frac{\delta}{D} \leq 6.25$. For all tests the undisturbed boundary layer at the injection station was fully turbulent. Vertical nondimensional pressure, velocity, concentration profiles, and total-pressure recovery results are presented. Results of this investigation illustrate a distinct increase in both the secondary jet penetration and the mixing rate with increasing δ/D .

INTRODUCTION

One type of fuel-injector design for scramjet combustors is the flush wall-mounted jet. This type of fuel injector normally is designed by empirical relation based on the data of numerous investigators. (For example, see refs. 1 to 15.) The investigations reported in the literature have not evaluated the effect on the mixing of the thickness of the boundary layer on the wall. In view of the complex interactions between the jet and boundary layer which are illustrated in the literature, the ratio of boundary-layer thickness to jet diameter is expected to be an important parameter. For instance, several investigations (see refs. 16 and 17) have shown that the properties of the boundary layer at the injection location have a measurable effect on this type of jet interaction.

The present preliminary investigation was designed to evaluate the effect of the magnitude of the ratio of boundary-layer thickness to jet diameter on the mixing performance. Tests were performed on a flat-plate model with sonic injection of hydrogen from a single normal jet into a fully developed turbulent boundary layer. Mixing region surveys were made at a station 120 injector diameters downstream of the jet for three separate configurations and compared with results from references 9 and 12. The effects of the ratio of boundary-layer thickness to jet diameter on jet penetration and mixing rate were measured and methods of correlating the data were determined.

SYMBOLS

A	area
b	profile shape factor (fig. 11)
C_D	discharge coefficient
D	jet diameter, cm
d^*	effective jet diameter, $D\sqrt{C_D}$, cm
H_2	hydrogen gas
ℓ	location of injector from leading edge, cm
M	Mach number
P	jet penetration, maximum height of $x_{H_2} = 0.005$ contour, cm
p	pressure, N/m ²
p_{eb}	effective back pressure, N/m ²
p_R	pressure recovery
q	dynamic pressure, N/m ²
R_X	Reynolds number based on X from plate leading edge
T	temperature, K
V	velocity, m/sec
X	longitudinal coordinate, cm
x_{H_2}	hydrogen mole fraction
Y	lateral coordinate, measured across plate from center line, cm

y_{H_2}	hydrogen mass fraction
Z	vertical coordinate, cm
α	hydrogen flow rate per unit area, $\rho V y_{H_2}$, kg/m ² -sec
β	airflow rate, per unit area, $\rho V (1 - y_{H_2})$, kg/m ² -sec
δ	boundary-layer thickness at jet station, cm
θ	boundary-layer momentum thickness, cm
ρ	density, kg/m ³

Subscripts:

A	mass-averaged undisturbed airflow condition
j	secondary jet condition
M	location of $y_{H_2, \max}$
max	maximum value in mixing region
0	point on vertical survey where $x_{H_2} = 0.005$
t	total condition
∞	free-stream condition

A bar over a symbol denotes a mass-averaged value.

MODEL AND FACILITY

Wind Tunnel and Model

The experiments were conducted in a Mach number 4.05, 22.84-cm-square wind tunnel with injection of hydrogen from a flat plate which spanned the test section. A sketch of the plate, locating the injection stations and defining the coordinate system, is presented in figure 1(a). Figure 1(b) presents details and the measured discharge

coefficients C_D of the circular injectors used in this study. Fuel was injected at the 18.6-cm upstream station for the test in reference 9 and at the 24-cm station for the present tests and the test in reference 12.

Instrumentation

Probes.- The pitot and static survey probes used in all these experiments are illustrated in figure 2. Probe actuator limitations required yawing the probes for lateral surveys; however, the maximum yaw angle was held to a relatively small angle (about 10°). The diameters of the probe static orifices were 0.203 mm; and the orifices were located 14 probe diameters from the probe tips. The pitot probe, a flattened hypodermic needle, was used to collect gas samples from the hydrogen-air mixing region for analysis by a gas chromatograph.

Gas sampling system.- A schematic of the gas sampling system is presented in figure 3. The heart of this system was a Control Data on-line process gas chromatograph which measures only hydrogen volume fraction. The chromatograph was tied into the hydrogen supply line and the pitot probe by a system of electrically operated valves. Pure hydrogen from the supply line was used to check the full-scale reading during each test. Other instrumentation used in these tests is also illustrated in this sketch (fig. 3).

Test Conditions

The test conditions are presented in the following table:

Test	D, cm	$P_{t,\infty}$, MN/m ²	$P_{t,j}$, MN/m ²	q_j/q_∞	ℓ , cm	δ/D
1	0.25	1.72	0.328	0.978	24.0	1.25
2	.05	1.72	.325	.973	24.0	6.25
3	.10	1.38	.271	1.006	24.0	3.16
4 (ref. 9)	.10	1.38	.270	1.005	18.6	2.51
5 (ref. 12)	.12	1.72	.335	1.001	24.0	2.58

All tests were run at a tunnel total pressure of either 1.38 or 1.72 MN/m² and a corresponding jet total pressure to produce a ratio of jet to free-stream dynamic pressure of unity. For each test the jet was sonic and underexpanded. Injector diameter, injector position, and free-stream total-pressure variations combine to produce different ratios of boundary-layer thickness to jet diameter δ/D as listed in the table. A theoretical boundary-layer thickness was used for this parameter; the theoretical solution is discussed in detail in a later section.

Test Procedure

The experimental results were reduced from survey data taken in the hydrogen-air mixing region 120 injector diameters downstream of the injection station. Surveys consisted of one vertical center-line survey and three horizontal surveys of hydrogen mole fraction, pitot pressure, and static pressure. Since pitot- and static-pressure measurements were made during separate tests, both measurements were nondimensionalized by free-stream total pressure before being included in the data-reduction program. (See appendix A.)

THEORETICAL BOUNDARY LAYER

Theoretically determined boundary-layer parameters were used in this study because it is difficult to obtain accurate measurements of very small boundary layers ($\delta \approx 0.3$ cm) and the development of the turbulent boundary layer in this facility had been predicted accurately in other investigations. The theoretical boundary layer was determined by using an integral transition and turbulent boundary-layer program developed by Pinckney. (See ref. 18.) The laminar boundary layer was predicted by an ordinary flat-plate solution with friction coefficient determined by Eckert's flat-plate reference temperature method. (See ref. 19.) Transition was assumed to start at the point where $R_X = 2.9 \times 10^6$, a value which was based on extensive boundary-layer tests performed in the facility on other flat-plate models.

Theoretical nondimensional boundary-layer velocity and total-pressure profiles at the injection station are presented in figure 4. These profiles represent a fully turbulent boundary layer for each case. Also included are values of the theoretically determined boundary-layer and momentum thicknesses. All boundary-layer parameters have been nondimensionalized by the jet diameter D . For this study, boundary-layer thickness δ corresponds to the point where the theoretical velocity is 99 percent of the free-stream value.

RESULTS AND DISCUSSION

Reduced survey data (appendix A) were used to construct flow contours (appendix B) of the mixing region. These contours are used to define three mixing parameters: jet penetration, mixing rate, and jet-induced interference. These mixing parameters are analyzed in the remaining discussion.

Penetration

Penetration has been correlated in this study by two characteristics of the hydrogen volume fraction contour. These characteristics are denoted by P/D and $(Z/D)_M$, corresponding to

P/D vertical height from the plate to the highest point on the $x_{H_2} = 0.005$ contour (outer edge of mixing region, see appendix B)

$(Z/D)_M$ vertical height from the plate to the point of maximum hydrogen concentration

Both penetration parameters are presented in figure 5 as a function of the ratio of boundary-layer thickness to jet diameter δ/D . On this and subsequent figures, the data points used from references 9 and 12 are flagged or designated. The trends of the data indicate that both P/D and $(Z/D)_M$ increase as δ/D becomes larger. The parameter P/D is a weak function of δ/D :

$$\frac{P}{D} \propto \left(\frac{\delta}{D}\right)^{0.0574} \quad (1)$$

However, the value of $(Z/D)_M$ increases by nearly 75 percent in the range $1.25 \leq \frac{\delta}{D} \leq 3.25$. The magnitude of these increases warrants inclusion of δ/D dependence in any jet-penetration correlation.

The penetration correlation of equation (1) agrees with results presented in reference 17. These results were obtained over a smaller range of δ/D and most of the penetration measurements were made relatively close to the injector. The data presented in reference 17, which include results from references 9 and 12, are correlated by

$$\frac{P}{D} = 2.96 \left(\frac{p_{t,j}}{p_{eb}}\right)^{0.405} M_j^{0.163} \left(\frac{X}{d^*} + 0.5\right)^{0.204} \left(\frac{\theta}{d^*}\right)^{0.141} \quad (2)$$

Since these results were all obtained with fully turbulent boundary layers, the boundary-layer thickness is proportional to the boundary-layer momentum thickness or

$$\frac{P}{D} \propto \left(\frac{\delta}{D}\right)^{0.141} \quad (3)$$

This proportionality is nearly the same as that shown by the present data (eq. (1)) as illustrated by the dashed curve in figure 5. The absolute values from equation (2) were not plotted because of the uncertainty of extrapolating equation (2) to $\frac{X}{D} = 120$.

Several of the earlier wall injection and mixing investigations studied the effect of dynamic-pressure ratio on penetration. For instance, the results of reference 9 were correlated by

$$\frac{P}{D} = 3.87 \left(\frac{q_j}{q_\infty} \right)^{0.30} \left(\frac{X}{D} \right)^{0.143} = 3.87 \left[\left(\frac{q_j}{q_\infty} \right)^{2.1} \frac{X}{D} \right]^{0.143} \quad (4)$$

The dependence of jet penetration on δ/D , as shown by equation (1), can be included in equation (4) as shown by figure 6. This figure correlates the present data with the data from reference 9 by the following equation:

$$\frac{P}{D} = 4.20 \left(\frac{q_j}{q_\infty} \right)^{0.30} \left(\frac{\delta}{D} \right)^{0.0574} \left(\frac{X}{D} \right)^{0.143} = 4.20 \left[\left(\frac{q_j}{q_\infty} \right)^{2.1} \left(\frac{\delta}{D} \right)^{0.4} \frac{X}{D} \right]^{0.143} \quad (5)$$

Equation (5) corresponds to the solid line in figure 6. Present data points are solid symbols and data points from reference 9 are open symbols. All reference 9 data were at constant δ/D , and values of X/D and q_j/q_∞ ranged from 7 to 200 and 0.5 to 2.0, respectively. The dashed curve represents equation (4) simply expanded to account for δ/D . Equation (5) has the same slope as the dashed curve, but it correlates the present data points. This plot shows that the present data point from reference 9 has the largest deviation from the trends of the present data. This deviation is believed to be associated with the different jet geometry used for the reference 9 test. (See fig. 1(b).)

No satisfactory correlation for the maximum hydrogen concentration trajectory was presented in reference 9 because the trajectory tends to decrease in the near field (from $\frac{X}{D} = 7$ to about 20 to 30), and then increase with downstream distance. However, at $\frac{X}{D} = 120$, the height of the point of maximum hydrogen concentration in reference 9 can be correlated by

$$\left(\frac{Z}{D} \right)_M = 3.19 \left(\frac{q_j}{q_\infty} \right)^{0.214} \quad (6)$$

The straight-line correlation of the maximum concentration trajectory in figure 5 is likewise represented by

$$\left(\frac{Z}{D} \right)_M \propto \left(\frac{\delta}{D} \right)^{0.214} \quad (7)$$

Equations (6) and (7) are combined and used to plot the present data and the data at $\frac{X}{D} = 120$ from reference 9 in figure 7. The results are correlated by

$$\left(\frac{Z}{D} \right)_M = 2.62 \left(\frac{q_j}{q_\infty} \right)^{0.214} \left(\frac{\delta}{D} \right)^{0.214} \quad (8)$$

Because of the complex nature of $(Z/D)_M$ as mentioned previously, the effect of δ/D on the maximum concentration trajectory cannot be predicted over the entire mixing region without additional tests.

One indication of the extent of mixing between the jet and the free stream is the decay of the maximum hydrogen mass fraction, $y_{H_2, \max}$. Values of $y_{H_2, \max}$ for each test are presented in figure 8 as a function of the ratio of boundary-layer thickness to jet diameter δ/D . Data trends indicate that $y_{H_2, \max}$ is proportional to $(\delta/D)^{-0.345}$ at $\frac{X}{D} = 120$. Reference 9 data replotted in reference 8 showed $y_{H_2, \max}$ is proportional to $\left(\frac{X}{D}\right)^{-0.69} \left(\frac{q_j}{q_\infty}\right)^{0.345}$ in the downstream mixing region $\left(\frac{X}{D} \geq 30\right)$. Combining these correlations yields

$$y_{H_2, \max} = 1.031 \left(\frac{q_j}{q_\infty}\right)^{0.345} \left(\frac{\delta}{D}\right)^{-0.345} \left(\frac{X}{D}\right)^{-0.690} \quad (9)$$

The data from both reference 9 and the present test are presented in figure 9 to illustrate this correlation. Reference 9 data are represented by open symbols and the present cases, all at $\frac{X}{D} = 120$, are represented by solid symbols. Equation (9) which is simply an extension of the correlation used in reference 9 closely correlates the present data.

Pressure Recovery

The efficiency of each component of a ramjet engine is normally related directly or indirectly to the loss in total pressure or momentum of the airflow as it passes through that component. The interaction between a normal secondary jet and the combustor airflow produces significant total-pressure losses as a result of induced shocks in the airstream combined with the lack of jet streamwise (X) momentum. However, the jet-induced total-pressure losses would be partially compensated for by reduced-combustion total-pressure losses in the wake regions behind the jets. The pressure losses have been evaluated for the present data by calculating the total-pressure recovery defined by

$$p_R = \frac{\bar{p}_t \left(\text{at } \frac{X}{D} = 120 \right)}{\bar{p}_t \left(\text{at } \frac{X}{D} = 0 \right)} \quad (10)$$

where \bar{p}_t is the mass-weighted total pressure calculated by

$$\frac{\bar{p}_t}{p_{t, \infty}} = \frac{\int \rho V \frac{p_t}{p_{t, \infty}} d\left(\frac{A}{A_0}\right)}{\int \rho V d\left(\frac{A}{A_0}\right)} \quad (11)$$

at each station. The mass-weighted total pressure at station $\frac{X}{D} = 0$ was obtained by use of a stream tube area with the same shape and total airflow rate as the mixing region. The no-injection theoretical boundary layer at $\frac{X}{D} = 0$ was used for these calculations.

The pressure recovery results are presented in figure 10 along with the nondimensionalized mass-weighted total pressure at the injector and survey station. The recovery (circle symbol in fig. 10) is a constant value of 43 percent with the exception of the data for $\frac{\delta}{D} = 1.25$, which drops to 35 percent. A recovery of 43 percent is equivalent to the recovery across a two-dimensional shock with a turning of 28° in a Mach 4.05 airstream. It should be noted that the theoretical total-pressure losses associated with mixing of the normal H_2 jet with the air would be small compared with the shock losses since the weight flow of H_2 is less than 3 percent of the airflow.

CONCLUDING REMARKS

This investigation has shown that for normal sonic injection of hydrogen from a flat plate into a supersonic airflow, the mixing performance is dependent on the ratio of plate boundary-layer thickness to jet diameter δ/D and the magnitude of this dependence necessitates its inclusion in any empirical mixing models. The experimental results show that increasing δ/D increases penetration, both of the outer edge of the mixing region and of the point of maximum concentration, and the extent of mixing as measured by the maximum hydrogen concentration. The results also show that the normal jet mixing regions have relatively low pressure recoveries as a result, evidently, of the strong induced shock wave. In these relatively thick boundary-layer cases ($1.25 \leq \frac{\delta}{D} \leq 6.25$), only the smallest value of δ/D had a noticeably different (lower) pressure recovery than the other cases. Nondimensional boundary-layer correlating parameters presented extend previous flat-plate mixing performance correlations of jet penetration and maximum concentration decay.

Langley Research Center,
National Aeronautics and Space Administration,
Hampton, Va., March 25, 1974.

APPENDIX A

SURVEY DATA

One vertical and three horizontal surveys of the mixing region at an X/D station of 120 were performed for each case with measurements of hydrogen concentration, pitot pressure, and static pressure taken along each survey. A computer program was used to reduce the raw data to the desired results presented in table I. These tabulated results are in U.S. Customary Units, and the applicable nomenclature follows:

X	longitudinal coordinate, in.
Y	lateral coordinate, in.
Z	vertical coordinate, in.
D	jet orifice diameter, in.
QJ/QI	ratio of jet pressure to free-stream dynamic pressure
LAMDA	ratio of jet mass flux to free-stream mass flux
GAMMA	ratio of specific heats
RHOVJ	jet mass flow per unit area, slugs/ft ² -sec
K	mole fraction of injected gas
PT2X	survey pitot pressure, psia
PIX	static pressure, psia
MWX	molecular weight of survey gas sample
MX	Mach number
TTX	total temperature, °R
TX	static temperature, °R

APPENDIX A – Concluded

VX	velocity, ft/sec
RHOVX	mass flow per unit area, slugs/ft ² -sec
XI	ratio of injected gas mass flow per unit area at survey point to jet mass flow
GX	mass fraction of injected gas
RHOVX*(1-GX)	survey-point air mass flow per unit area
XIM	maximum XI
GXM	maximum GX
AIRMFM	maximum RHOVX*(1-GX)
AKXM	maximum K

Hydrogen concentration and total-pressure profile results from the vertical surveys are presented in figures 11 and 12, respectively. The hydrogen concentration profiles in figure 11 are divided into two regions, separated by the point of maximum hydrogen concentration. In the upper region the profile shape resembles coaxial mixing profiles; whereas in the lower region it is more uniform, since the plate restricts the mixing. Previous investigations have shown that, in the upper region, the profile shape is dependent on the downstream station but independent of dynamic-pressure ratio (refs. 9 and 12) or injection angle (ref. 7). On the other hand, the profile shape in the lower region is dependent on downstream distance, dynamic pressure, and injection angle. Although there is some variation in the profile shapes presented in figure 11, there is no evidence of a systematic effect of δ/D .

Nondimensional vertical total-pressure profiles are presented in figure 12 for each test and for a representative boundary-layer profile at the injector station. In figure 12 the height dimension is expressed as a ratio to the height of the outer edge of the mixing region or for the boundary-layer profile, to the boundary-layer thickness. Each mixing region profile exhibits a marked reduction in pressure recovery over the boundary-layer profile. Of course, the mixing region is considerably thicker than the boundary layer so the boundary-layer curve does not show the true extent of the pressure deficiency that is shown by the integrated pressure recovery. (See fig. 10.)

APPENDIX B

FLOW CONTOUR

Mixing region flow contours were constructed by cross plotting the vertical and horizontal survey data. Contours of hydrogen mass fraction, hydrogen flow rate, airflow rate, and mass-weighted total pressure $\left(\rho V \frac{p_t}{p_{t,\infty}}\right)$ are presented in figures 13 to 16, respectively. The mixing region edge corresponds to the $x_{H_2} = 0.005$ contour, denoted $y_{H_2} = 0$ in figure 13.

The hydrogen mass fraction contours (fig. 13) were used to determine the penetration and hydrogen mixing rate as discussed in the test. In addition, these contours show the effect of δ/D on hydrogen lateral spreading. One method of measuring the lateral spreading is to measure the width of the 10 percent of maximum hydrogen concentration contour at the vertical position (Z/D) of maximum concentration. Lateral locations of 10 percent of $y_{H_2,max}$ are noted in figure 13 by the vertical dashes on either side of $y_{H_2,max}$. By using this 10-percent procedure, these contours show a significant decrease in spreading from the largest δ/D case, $\frac{\delta}{D} = 6.25$, to the 3.16 case, and then a continued, but modest, decrease in spreading to the smaller δ/D conditions.

Hydrogen flow contours (fig. 14) were integrated to determine the accuracy of the sampling procedures by comparing the total hydrogen flow rate in the contours with the hydrogen flow rate measured by the orifice meter in the hydrogen supply line. Results of this integration show that 80 to 90 percent of the injected hydrogen was accounted for in the mixing region. This result is typical of this type of flat-plate mixing study.

Airflow contours (fig. 15) and mass-weighted total-pressure contours (fig. 16) were used to determine the total-pressure recovery, as discussed in the text. The airflow contours were used to determine the total airflow in the mixing region and to define the undisturbed airstream tube at the injector station which supplies air to the mixing region. The airflow contours also give an indication of the effect of the jet on the airflow. All mixing regions have relatively low airflow in the center (at the point of maximum concentration) and return toward a typical (but thick) boundary-layer distribution near the sides. The contours for the larger δ/D cases tend to simply decrease from the center outward, but the smaller δ/D cases show more flow distortion as indicated by the sharp dip from the center.

REFERENCES

1. Billig, F. S.; Orth, R. C.; and Lasky, M.: A Unified Approach to the Problem of Gaseous Jet Penetration Into a Supersonic Stream. AIAA Paper No. 70-93, Jan. 1970.
2. Chrans, Larry J.; and Collins, David J.: Stagnation Temperature and Molecular Weight Effects in Jet Interaction. AIAA J., vol. 8, no. 2, Feb. 1970, pp. 287-293.
3. Cohen, Leonard S.; Coulter, Lawrence J.; and Chiappetta, Louis: Hydrocarbon-Fueled Scramjet. Vol. VII Fuel Distribution Investigation. AFAPL-TR-68-146, Vol. VII, U.S. Air Force, Apr. 1970.
4. Collins, D. J.; Koch, L. N.; and Chambers, R. A.: An Investigation of Jet-Interaction. NPS-57C09101A, U.S. Naval Postgraduate School, Oct. 1, 1969. (Available from DDC as AD 864 693.)
5. Hersch, Martin, Povinelli, Louis S.; and Povinelli, Frederick P.: Optical Study of Sonic and Supersonic Jet Penetration From a Flat Plate Into a Mach 2 Airstream. NASA TN D-5717, 1970.
6. McClinton, Charles R.: The Effect of Injection Angle on the Interaction Between Sonic Secondary Jets and a Supersonic Free Stream. NASA TN D-6669, 1972.
7. Orth, R. C.; Schetz, J. A.; and Billig, F. S.: The Interaction and Penetration of Gaseous Jets in Supersonic Flow. NASA CR-1386, 1969.
8. Rogers, R. Clayton: Mixing of Hydrogen Injected From Multiple Injectors Normal to a Supersonic Airstream. NASA TN D-6476, 1971.
9. Rogers, R. Clayton: A Study of the Mixing of Hydrogen Injected Normal to a Supersonic Airstream. NASA TN D-6114, 1971.
10. Schetz, Joseph A.; Hawkins, Paul F.; and Lehman, Harry: Structure of Highly Under-expanded Transverse Jets in a Supersonic Stream. AIAA J., vol. 5, no. 5, May 1967, pp. 882-884.
11. Spaid, F. W.; Zukoski, E. E.; and Rosen, R.: A Study of Secondary Injection of Gases Into a Supersonic Flow. Tech. Rep. No. 32-834, Jet Propulsion Lab., California Inst. Technol., Aug. 1, 1966.
12. Torrence, Marvin G.: Concentration Measurements of an Injected Gas in a Supersonic Stream. NASA TN D-3860, 1967.
13. Torrence, Marvin G.: Effect of Injectant Molecular Weight on Mixing of a Normal Jet in a Mach 4 Airstream. NASA TN D-6061, 1971.
14. Vranos, A.; and Nolan, J. J.: Supersonic Mixing of a Light Gas and Air. Pratt & Whitney Aircraft, United Aircraft Corp., [1964].

15. Zukoski, Edward E.; and Spaid, Frank W.: Secondary Injection of Gases Into a Supersonic Flow. Jet Propulsion Center, California Inst. Technol., Oct. 1963.
16. Goldstein, R. J.; Eckert, E. R. G.; Eriksen, V. L.; and Ramsey, J. W.: Film Cooling Following Injection Through Inclined Circular Tubes. HTL TR No. 91, Heat Transfer Lab., Univ. of Minn., Nov. 1969. (Available as NASA CR-72612.)
17. Povinelli, Frederick P.; and Povinelli, Louis A.: Correlation of Secondary Sonic and Supersonic Gaseous Jet Penetration Into Supersonic Crossflows. NASA TN D-6370, 1971.
18. Pinckney, S. Z.: Method for Predicting Compressible Turbulent Boundary Layers in Adverse Pressure Gradients. NASA TM X-2302, 1971.
19. Eckert E. R. G.: Engineering Relations for Friction and Heat Transfer to Surfaces in High Velocity Flow. J. Aeronaut. Sci., vol. 22, no. 8, Aug. 1955, pp. 585-587.

TABLE I.- TABULATED DATA

Test 1 SURVEY 1-1-120V

QJ/Q1 = .9781 LAMDA = .5585

JET GAS MOL.WT. SPECIFIC HEAT GAMMA AVG. TOTAL TEMP. (DEG.R) TOTAL PRESS. (PSIA)
 TUNNEL GAS 2.016 3.4060 1.407 521 47.52
 29.000 .2400 1.399 531 249.72

RHCYJ = 1.3096E+00 XIM = 1.8906E-02 GXH = 3.3192E-02 AIRMFM = 2.2894E+00 AKXM = 3.3060E-01

Y/O	Z/D	K	PT2X	PIX	HMX	MX	TTX	TX	VX	RHOVX	XI	GX	RHOVX*(1-GX)	PRM
COORDINATES		REL FR.	PSIA	PSIA	MOL WT	MACH	-DEG.R.-		FT/SEC	SLG/SOFTSEC		MASS FR.	AIR MASS FLOW	
0.00	0.0000	.2457	3.000	1.685	22.37	.946	529	448	1.117.49	.2724	4.6041E-03	2.2138E-02	2.6634E-01	.0170
0.00	.6100	.2904	3.960	1.684	21.16	1.180	528	413	1.375.39	.3440	7.2733E-03	2.7691E-02	3.3446E-01	.0154
0.00	1.0000	.3145	6.420	1.652	20.51	1.619	528	346	1.754.61	.4982	1.1758E-02	3.0909E-02	4.8278E-01	.0287
0.00	1.5000	.3256	7.650	1.642	20.22	1.797	528	320	1.887.36	.5670	1.4056E-02	3.2466E-02	5.4857E-01	.0376
0.00	2.0000	.3306	8.660	1.643	20.08	1.925	528	302	1.972.48	.6234	1.5799E-02	3.3193E-02	6.0267E-01	.0459
0.00	2.5000	.3306	9.820	1.645	20.08	2.062	528	285	2.049.27	.6892	1.7467E-02	3.3193E-02	6.6628E-01	.0568
0.00	3.0000	.3165	11.210	1.636	20.46	2.223	528	265	2.111.31	.7728	1.8404E-02	3.1188E-02	7.4873E-01	.0726
0.00	3.5000	.3015	12.450	1.630	20.86	2.357	528	250	2.151.48	.8492	1.8892E-02	2.9136E-02	8.2441E-01	.0892
0.00	4.0000	.2867	13.420	1.625	21.26	2.457	528	239	2.172.99	.9110	1.8906E-02	2.7178E-02	8.8627E-01	.1040
0.00	4.5000	.2671	14.390	1.620	21.90	2.550	528	229	2.177.49	.9764	1.8050E-02	2.4227E-02	9.5270E-01	.1190
0.00	5.0000	.2351	15.170	1.619	22.66	2.627	529	222	2.168.90	1.0396	1.6602E-02	2.0916E-02	1.0178E+00	.1349
0.00	5.6100	.1951	16.320	1.620	23.73	2.730	529	212	2.153.68	1.1306	1.4310E-02	1.6576E-02	1.1118E+00	.1581
0.00	6.0000	.1496	17.700	1.622	24.96	2.847	530	202	2.136.05	1.2411	1.1452E-02	1.2005E-02	1.2261E+00	.1893
0.00	6.5000	.1025	19.960	1.620	26.23	3.033	530	187	2.133.97	1.4083	8.4737E-03	7.4798E-03	1.3972E+00	.2505
0.00	7.0000	.0619	23.000	1.620	27.33	3.265	530	169	2.144.14	1.6230	5.6580E-03	4.5633E-03	1.6164E+00	.3530
0.00	7.5000	.0324	26.380	1.620	28.13	3.505	531	154	2.160.50	1.8565	3.2904E-03	2.3211E-03	1.8522E+00	.4988
0.00	8.0000	.0136	29.220	1.639	28.63	3.672	531	144	2.169.96	2.0528	1.4968E-03	9.5491E-04	2.0500E+00	.6306
0.00	8.5000	.0042	30.860	1.685	28.89	3.724	531	141	2.168.78	2.1707	4.8901E-04	2.9503E-04	2.1701E+00	.7050
0.00	9.0000	.0008	31.810	1.700	28.98	3.765	531	139	2.171.75	2.2357	1.0032E-04	5.8764E-05	2.2356E+00	.7529
0.00	9.5000	0.0000	32.600	1.723	29.00	3.786	531	137	2.174.14	2.2894	0.	0.	2.2894E+00	.7860
0.00	1.0000	.3286	0.330	1.641	20.13	1.886	528	308	1.946.13	.6051	1.5202E-02	3.2901E-02	5.8521E-01	.0431
0.00	2.3900	.3306	5.260	1.647	20.08	1.996	528	293	2.012.66	.6578	1.6671E-02	3.3193E-02	6.3593E-01	.0513
-0.00	2.0900	.3326	8.600	1.642	20.02	1.919	527	303	1.969.22	.6196	1.5861E-02	3.3486E-02	5.9889E-01	.0454
-9.35	2.0900	.0102	17.230	1.358	28.73	3.081	530	183	2.050.78	1.2664	6.9042E-04	7.1321E-04	1.2655E+00	.2255
-10.60	2.0900	0.0000	17.610	1.248	29.00	3.255	530	170	2.079.19	1.2817	0.	0.	1.2817E+00	.2682
-9.76	2.0900	.0042	17.720	1.297	28.89	3.201	530	174	2.071.89	1.2928	2.9155E-04	2.9503E-04	1.2924E+00	.2575
-7.86	2.0900	.0102	17.800	1.392	28.73	3.093	530	182	2.053.66	1.3068	7.1248E-04	7.1321E-04	1.3059E+00	.2355
-6.45	2.0900	.0178	15.510	1.465	28.52	2.803	530	206	1.987.82	1.1667	1.1237E-03	1.2599E-03	1.1653E+00	.1600
-5.14	2.0900	.0136	21.420	1.445	28.63	3.339	530	164	2.108.93	1.5397	1.1239E-03	9.5491E-04	1.5382E+00	.3508
-3.92	2.0900	.0247	23.200	1.534	28.33	3.374	530	162	2.126.49	1.6550	2.2196E-03	1.7545E-03	1.6521E+00	.3915
-2.64	2.0900	.0436	18.190	1.621	26.47	2.889	529	198	2.085.22	1.3081	7.1287E-03	7.1289E-03	1.2988E+00	.2017
-1.37	2.0900	.2044	13.970	1.645	23.38	2.444	528	235	2.086.40	.9094	1.3589E-02	1.7968E-02	9.7160E-01	.1115
-0.00	2.0900	.3165	9.640	1.642	20.46	2.044	527	287	2.018.51	.6857	1.6348E-02	3.1188E-02	6.6433E-01	.0551
.90	2.0900	.3245	9.200	1.640	20.24	1.993	527	293	2.001.36	.6570	1.6234E-02	3.2322E-02	6.3580E-01	.0509
1.84	2.0900	.2612	11.920	1.643	21.95	2.293	527	257	2.068.90	.8422	1.5442E-02	2.3985E-02	8.2204E-01	.0813
2.88	2.0900	.1588	15.840	1.650	24.71	2.462	528	218	2.087.84	1.1290	1.1182E-02	1.2956E-02	1.1144E+00	.1450
4.01	2.0900	.0566	20.440	1.613	27.47	3.078	529	183	2.095.27	1.4704	4.6708E-03	4.1555E-03	1.4643E+00	.2668
5.05	2.0900	.0212	22.390	1.569	28.43	3.274	530	169	2.103.34	1.6116	1.8555E-03	1.5062E-03	1.6092E+00	.3465
6.55	2.0900	.0119	20.320	1.468	28.68	3.223	530	172	2.083.70	1.4747	9.3998E-04	8.3381E-04	1.4735E+00	.3008
7.99	2.0900	.0144	14.820	1.468	28.61	2.734	530	213	1.965.22	1.1250	8.7341E-04	1.0157E-03	1.1238E+00	.1442
9.02	2.0900	.0182	16.210	1.429	28.73	2.906	530	197	2.008.29	1.2109	6.6015E-04	7.1321E-04	1.2100E+00	.1825
10.95	2.0900	.0051	16.750	1.335	28.66	3.063	530	184	2.041.92	1.2359	3.3481E-04	3.5440E-04	1.2354E+00	.2159
12.97	2.0900	.0034	15.810	1.310	29.91	3.002	530	189	2.025.85	1.1739	2.1158E-04	2.3578E-04	1.1736E+00	.1933
12.09	2.0900	.0017	15.820	1.290	28.95	3.027	530	187	2.030.31	1.1728	1.0548E-04	1.1765E-04	1.1727E+00	.1976
12.54	2.0900	0.0000	16.000	1.279	29.00	3.058	530	185	2.036.14	1.1837	0.	0.	1.1837E+00	.2054

TABLE I.- TABULATED DATA - Continued

Test 1 - Concluded

V/D	Z/D	K	PT2X	PIX	MWX	MX	TX	TX	VX	RHOVX	XI	GX	RHOVX*(1-GX)	PRM
COORDINATES		MOL FR.	PSIA	PSIA	MOL WT	MACH	-DEG.R.-		FT/SEC	SLG/SQFTSEC		MASS FR.	AIR MASS FLOW	
-0.00	1.0900	.3175	6.450	1.640	20.43	1.630	527	343	1764.37	.4987	1.1944E-02	3.1328E-02	4.8312E-01	.0292
-12.90	1.0900	0.0000	10.190	1.344	29.00	2.349	530	252	1826.63	.8178	0.	0.	8.1783E-01	.0726
-11.52	1.0900	.0008	10.200	1.345	28.98	2.349	530	252	1827.44	.8183	3.6757E-05	5.8764E-05	8.1824E-01	.0727
-10.05	1.0900	.0025	10.400	1.365	28.93	2.355	530	252	1831.01	.8330	1.1248E-04	1.7665E-04	8.3283E-01	.0745
-8.70	1.0900	.0043	10.310	1.417	28.75	2.297	530	258	1814.97	.8303	4.1451E-04	6.5310E-04	8.2974E-01	.0707
-7.39	1.0900	.0170	10.640	1.478	28.54	2.284	530	259	1816.28	.8556	7.8392E-04	1.1986E-03	8.5454E-01	.0722
-5.94	1.0900	.0255	10.220	1.479	28.31	2.234	530	265	1803.68	.8250	1.1458E-03	1.8170E-03	8.2347E-01	.0668
-4.58	1.0900	.0255	14.600	1.533	28.31	2.651	530	220	1950.69	1.1131	1.5460E-03	1.8170E-03	1.1111E+00	.1126
-3.02	1.0900	.0558	12.150	1.600	27.50	2.350	529	252	1875.38	.9500	2.9686E-03	4.0880E-03	9.4609E-01	.0867
-1.70	1.0900	.1460	10.290	1.620	25.06	2.134	529	276	1870.02	.7957	7.1418E-03	1.1742E-02	7.8631E-01	.0526
-0.00	1.0900	.2808	7.780	1.640	21.42	1.815	527	317	1843.87	.5916	1.1947E-02	2.6419E-02	5.7593E-01	.0487
1.65	1.0900	.2700	8.220	1.640	21.72	1.872	527	310	1865.65	.6219	1.1915E-02	2.5063E-02	6.0632E-01	.0422
3.02	1.0900	.1551	10.470	1.622	24.41	2.153	528	274	1887.71	.8031	7.7386E-03	1.2605E-02	7.9300E-01	.0645
4.39	1.0900	.0610	12.020	1.605	27.35	2.333	529	254	1873.43	.9397	3.2294E-03	4.4950E-03	9.3563E-01	.0846
5.89	1.0900	.0281	13.200	1.571	28.24	2.481	530	238	1897.82	1.0268	1.5737E-03	2.0050E-03	1.0247E+00	.1044
7.25	1.0900	.0229	12.000	1.506	28.38	2.412	530	245	1869.08	.9445	1.1769E-03	1.6301E-03	9.4297E-01	.0838
8.70	1.0900	.0204	9.390	1.496	28.45	2.121	530	279	1751.85	.7741	8.5464E-04	1.4444E-03	7.7297E-01	.0556
10.14	1.0900	.0119	10.300	1.441	28.68	2.275	530	261	1808.62	.8313	5.2984E-04	8.3381E-04	8.3058E-01	.0594
11.00	1.0900	.0034	9.300	1.400	28.91	2.187	530	271	1766.27	.7641	1.3772E-04	2.3578E-04	7.6394E-01	.0535
13.18	1.0900	0.0000	10.290	1.379	29.00	2.329	530	254	1819.19	.8283	0.	0.	8.2828E-01	.0722
-0.00	5.8900	.1718	16.920	1.617	24.36	2.785	534	209	2153.32	1.1745	1.2837E-02	1.4214E-02	1.1578E+00	.1722
-5.00	5.8900	0.0000	32.390	1.414	29.00	4.176	536	120	2236.41	2.2212	0.	0.	2.2212E+00	1.0886
-3.02	5.8900	.0085	30.170	1.498	28.77	3.910	536	132	2210.57	2.0871	9.5182E-04	5.9311E-04	2.0859E+00	.8102
-1.02	5.8900	.0307	26.540	1.565	28.17	3.579	536	151	2181.90	1.8517	3.1242E-03	2.1943E-03	1.8476E+00	.5365
-1.04	5.8900	.0990	20.680	1.609	26.33	3.101	535	183	2156.61	1.4463	8.4264E-03	7.5774E-03	1.4353E+00	.2759
-0.99	5.8900	.1469	18.250	1.618	25.04	2.897	535	199	2157.08	1.2691	1.1542E-02	1.1828E-02	1.2541E+00	.2042
-0.00	5.8900	.1681	17.450	1.617	24.46	2.830	534	205	2162.53	1.2080	1.2864E-02	1.3850E-02	1.1912E+00	.1845
1.09	5.8900	.1460	18.050	1.615	25.06	2.683	535	201	2152.18	1.2575	1.1354E-02	1.1742E-02	1.2428E+00	.1996
2.03	5.8900	.0901	20.600	1.620	26.57	3.084	535	184	2143.00	1.4492	7.6144E-03	6.8334E-03	1.4393E+00	.2708
3.02	5.8900	.0350	25.000	1.617	28.04	3.413	536	161	2156.20	1.7601	3.4001E-03	2.5124E-03	1.7556E+00	.4374
3.96	5.8900	.0059	29.600	1.545	28.86	3.811	536	137	2193.84	2.0607	6.5582E-04	4.1389E-04	2.0599E+00	.7306
4.90	5.8900	0.0000	31.000	1.462	29.00	4.014	536	127	2216.19	2.1416	0.	0.	2.1416E+00	.9097

TABLE I.- TABULATED DATA - Continued

Test 2 SURVEY 2-1-120V

QJ/QI = .9736 LAMDA = .5547

JFT GAS	MOL.WT.	SPECIFIC HEAT	GAMMA	AVG.TOTAL TEMP.(DEG.R)	TOTAL PRESS.(PSIA)
TUNNEL GAS	29.016	3.4130	1.406	536	47.12
	29.000	.2400	1.399	545	248.92

RHQVJ = 1.2799E+00 XIM = 1.0337E-02 GXM = 1.9177E-02 AIRMFH = 2.2101E+00 AKXP = 2.1952E-01

Y/D	Z/D	K	PT2X	P1X	MX	MX	TTX	TX	VX	RHQVX	XI	GX	RHOVX*(1-GX)	PRM
COORDINATES	MOL FR.	PSIA	PSIA	MOL WT	MACH	-DEG.R-	FT/SEC	SLG/SCFTSEC	MASS FR.	AIR MASS FLOW				
0.00	0.0000	.1679	3.050	1.535	24.47	1.041	544	447	1173.06	.2858	3.0886E-03	1.3831E-02	2.8107E-01	.0123
0.00	1.4000	.1688	3.100	1.535	24.44	1.054	543	445	1186.21	.2901	3.1559E-03	1.3925E-02	2.8604E-01	.0125
0.00	2.8000	.1682	6.050	1.386	23.92	1.732	543	339	1721.26	.4872	6.0357E-03	1.5857E-02	4.7545E-01	.0289
0.00	3.2000	.2057	7.750	1.648	23.45	1.807	543	328	1784.00	.6022	8.4058E-03	1.7689E-02	5.9748E-01	.0325
0.00	4.6000	.2195	8.250	1.989	23.08	1.682	543	347	1719.85	.6599	9.8872E-03	1.9177E-02	6.4723E-01	.0384
0.00	6.0000	.1989	9.760	2.006	23.63	1.842	543	323	1797.76	.7634	1.0119E-02	1.6966E-02	7.5048E-01	.0494
0.00	7.4000	.1195	14.250	1.706	25.78	2.473	544	245	2009.70	1.0465	7.4424E-03	9.3474E-03	1.0367E+00	.1122
0.00	8.8000	.0570	20.150	1.685	27.46	2.978	544	196	2100.45	1.4422	4.7105E-03	4.1807E-03	1.4361E+00	.2420
0.00	9.2000	.0336	23.950	1.680	28.09	3.272	545	174	2144.93	1.6904	3.1839E-03	2.4108E-03	1.6063E+00	.3712
0.00	10.6000	.0176	27.750	1.662	28.53	3.518	545	157	2176.17	1.9043	1.8509E-03	1.2440E-03	1.9019E+00	.5226
0.00	12.0000	.0053	30.150	1.645	28.86	3.725	545	145	2198.46	2.0522	6.0051E-04	3.6763E-04	2.0914E+00	.6918
0.00	11.2000	.0024	31.400	1.640	28.93	3.810	545	140	2208.71	2.1713	3.1062E-04	1.8322E-04	2.1709E+00	.7746
0.00	11.7000	0.0000	32.120	1.638	29.00	3.856	545	137	2212.95	2.2181	0.	0.	2.2181E+00	.8749
0.00	6.2000	.2146	8.200	1.924	23.21	1.719	543	341	1738.62	.6525	9.5014E-03	1.8639E-02	6.4030E-01	.0388
0.00	5.2000	.2166	8.800	2.076	23.16	1.703	543	343	1730.63	.7018	1.0337E-02	1.8853E-02	6.8856E-01	.0414
-0.00	4.4000	.2185	8.180	1.973	23.10	1.682	545	348	1721.07	.6538	9.7403E-03	1.9069E-02	6.4131E-01	.0381
-10.13	4.4000	0.0000	15.160	1.604	29.00	2.641	547	229	1955.43	1.1525	0.	0.	1.1525E+00	.1371
-9.01	4.4000	.0035	14.990	1.620	28.91	2.611	547	232	1949.33	1.1418	2.1816E-04	2.4456E-04	1.1415E+00	.1323
-8.16	4.4000	.0070	15.000	1.644	28.81	2.592	547	234	1946.29	1.1434	4.3881E-04	4.9122E-04	1.1428E+00	.1303
-7.04	4.4000	.0158	15.160	1.656	28.67	2.564	547	236	1945.05	1.1545	1.0081E-03	1.1172E-03	1.1537E+00	.1287
-5.91	4.4000	.0318	15.700	1.892	28.14	2.422	547	252	1910.51	1.1711	2.0851E-03	2.2789E-03	1.1684E+00	.1152
-4.79	4.4000	.0542	14.830	2.060	27.54	2.284	546	268	1877.69	1.1535	3.5789E-03	3.9711E-03	1.1489E+00	.1011
-3.52	4.4000	.0826	13.820	2.071	26.50	2.175	546	281	1866.78	1.0580	5.8206E-03	7.0414E-03	1.0506E+00	.0857
-2.25	4.4000	.1478	11.240	1.940	25.01	2.030	545	299	1851.06	.8705	8.1025E-03	1.1914E-02	8.6012E-01	.0639
-1.99	4.4000	.1989	8.920	1.923	23.63	1.793	545	331	1771.48	.7038	9.3286E-03	1.6966E-02	6.6184E-01	.0440
-0.00	4.4000	.2185	8.190	1.963	23.10	1.688	545	347	1725.06	.6537	9.7350E-03	1.9069E-02	6.4123E-01	.0383
1.13	4.4000	.1999	8.850	2.020	23.61	1.736	545	340	1737.36	.7064	9.4202E-03	1.7068E-02	6.9436E-01	.0423
2.39	4.4000	.1459	11.020	2.029	25.06	1.959	545	309	1817.07	.8657	7.9376E-03	1.1736E-02	8.5549E-01	.0599
3.52	4.4000	.1046	12.610	1.881	26.18	2.198	546	278	1888.04	.9701	6.1053E-03	8.0551E-03	9.6230E-01	.0806
4.50	4.4000	.0678	13.970	1.779	27.17	2.393	546	255	1932.56	1.0624	4.1781E-03	5.0334E-03	1.0571E+00	.1035
5.77	4.4000	.0345	15.130	1.722	28.07	2.540	547	239	1954.19	1.1461	2.2180E-03	2.4770E-03	1.1433E+00	.1260
6.93	4.4000	.0176	15.610	1.705	28.53	2.597	547	233	1957.26	1.1835	1.1503E-03	1.2440E-03	1.1820E+00	.1361
7.88	4.4000	.0070	15.700	1.693	28.81	2.614	547	231	1953.41	1.1935	4.5804E-04	4.9122E-04	1.1929E+00	.1389
8.72	4.4000	.0035	15.600	1.692	28.91	2.614	547	231	1950.35	1.1878	2.2695E-04	2.4456E-04	1.1875E+00	.1381
9.57	4.4000	.0009	15.220	1.679	28.98	2.583	547	235	1938.02	1.1647	5.5456E-05	6.0945E-05	1.1646E+00	.1313
10.55	4.4000	0.0000	15.040	1.675	29.00	2.570	547	236	1933.06	1.1532	0.	0.	1.1532E+00	.1284

TABLE I.- TABULATED DATA - Continued

Test 2 - Concluded

Y/D	Z/D	K	PT2X	PIX	MWX	MX	TTX	TC	VX	RHOVX	XI	GX	RHOVX*(1-GX)	PRM
COORDINATES	MOL FR.	PSIA	PSIA	MOL WT	MACH	-DEG.R...	FT/SEC	SLG/SOFTSEC	MASS FR.	AIR MASS FLOW				
-0.00	2.3000	.1872	5.600	1.449	23.95	1.614	543	357	1643.78	.4633	5.6443E-03	1.5758E-02	4.5602E-01	.0253
-10.69	2.3000	0.0000	8.800	1.677	29.00	1.922	547	315	1663.99	.7474	0.	0.	7.4745E-01	.0467
-9.29	2.3000	.0053	8.550	1.719	28.06	1.866	547	321	1645.31	.7326	2.0820E-04	2.6763E-04	7.3233E-01	.0439
-7.88	2.3000	.0158	8.590	1.773	28.57	1.838	547	320	1638.41	.7367	6.3629E-04	1.1172E-03	7.3590E-01	.0434
-6.76	2.3000	.0409	8.800	1.811	28.17	1.841	546	320	1651.25	.7451	1.2817E-03	2.2131E-03	7.4747E-01	.0445
-5.55	2.3000	.0524	9.000	1.782	27.59	1.801	546	320	1689.25	.7525	2.2292E-03	3.8322E-03	7.4958E-01	.0466
-4.25	2.3000	.0806	9.120	1.521	26.82	2.068	545	299	1805.78	.7264	3.4022E-03	6.0587E-03	7.2197E-01	.0532
-3.25	2.3000	.1120	8.790	1.380	25.98	2.138	545	285	1866.07	.6812	4.5791E-03	8.6949E-03	6.7531E-01	.0538
-2.25	2.3000	.1374	8.060	1.476	25.29	1.964	544	307	1805.30	.6362	5.3852E-03	1.0950E-02	6.2920E-01	.0439
-1.13	2.3000	.1650	6.600	1.540	24.55	1.714	543	342	1688.18	.5404	5.6813E-03	1.3950E-02	5.3311E-01	.0312
-0.15	2.3000	.1872	5.600	1.460	23.95	1.607	543	358	1639.00	.4641	5.6534E-03	1.5758E-02	4.5676E-01	.0252
1.15	2.3000	.1679	6.400	1.574	24.47	1.663	543	350	1658.44	.5292	5.6584E-03	1.3831E-02	5.2188E-01	.0295
2.15	2.3000	.1383	7.590	1.775	25.27	1.712	544	343	1661.59	.6305	5.3791E-03	1.1037E-02	6.2350E-01	.0358
3.15	2.3000	.1074	8.250	1.866	26.10	1.765	545	335	1657.57	.6911	4.4307E-03	8.2936E-03	6.8532E-01	.0396
4.15	2.3000	.0751	8.680	1.860	26.97	1.799	545	331	1662.81	.7301	3.1692E-03	5.6152E-03	7.2598E-01	.0429
5.19	2.3000	.0457	9.090	1.814	27.66	1.862	546	323	1676.70	.7640	2.1409E-03	3.6250E-03	7.6119E-01	.0465
6.33	2.3000	.0310	9.370	1.804	28.14	1.911	546	316	1688.51	.7863	1.3852E-03	2.2789E-03	7.8447E-01	.0494
7.46	2.3000	.0176	9.590	1.765	28.53	1.959	547	309	1701.84	.8024	7.7168E-04	1.2440E-03	8.0138E-01	.0521
8.44	2.3000	.0088	9.360	1.742	28.76	1.947	547	311	1689.18	.7880	3.7488E-04	6.1534E-04	7.8756E-01	.0505
9.57	2.3000	.0035	8.940	1.727	28.91	1.907	547	317	1665.30	.7603	1.4375E-04	2.4456E-04	7.6013E-01	.0470
10.41	2.3000	.0009	8.740	1.719	28.98	1.888	547	320	1653.68	.7470	3.5193E-05	6.0945E-05	7.4693E-01	.0454
11.39	2.3000	0.0000	8.750	1.709	29.00	.896	547	318	1656.80	.7470	0.	0.	7.4703E-01	.0457
-0.00	8.2000	.0870	16.800	1.692	26.65	2.710	546	221	2059.08	1.2182	6.1844E-01	6.5841E-03	1.2082E+00	.1608
-7.46	8.2000	0.0000	27.430	1.575	29.00	3.874	548	151	2182.91	1.9141	0.	0.	1.9141E+00	.5774
-6.62	8.2000	.0018	27.710	1.586	28.95	3.601	548	153	2180.71	1.9000	1.7905E-04	1.2202E-04	1.8998E+00	.5614
-5.91	8.2000	.0044	28.840	1.615	28.88	3.547	548	156	2173.19	1.8790	4.4408E-04	3.0603E-04	1.8784E+00	.5264
-4.93	8.2000	.0105	26.310	1.640	28.72	3.478	548	160	2161.69	1.8446	1.0542E-03	7.4000E-04	1.8432E+00	.4802
-3.94	8.2000	.0220	25.000	1.640	28.41	3.388	547	166	2161.78	1.7547	2.1108E-03	1.5635E-03	1.7520E+00	.4288
-2.96	8.2000	.0407	22.940	1.641	27.90	3.210	547	179	2143.48	1.5899	3.6153E-03	2.9444E-03	1.5852E+00	.3312
-2.11	8.2000	.0560	20.450	1.642	27.49	3.047	547	151	2120.91	1.4522	4.6102E-03	4.1107E-03	1.4462E+00	.2609
-1.27	8.2000	.0780	18.250	1.657	26.95	2.861	546	207	2092.42	1.3068	5.7412E-03	5.6887E-03	1.2993E+00	.1985
-0.42	8.2000	.0961	16.880	1.662	26.84	2.739	546	218	2067.24	1.2189	6.1244E-03	6.4003E-03	1.2106E+00	.1656
1.28	8.2000	.0880	16.780	1.667	26.63	2.729	546	219	2065.95	1.2116	6.2317E-03	6.6559E-03	1.2035E+00	.1632
1.13	8.2000	.0806	17.440	1.667	26.82	2.785	546	214	2075.31	1.2560	5.8769E-03	6.0587E-03	1.2484E+00	.1778
1.97	8.2000	.0606	19.440	1.667	27.37	2.945	547	200	2099.62	1.3878	4.7826E-03	4.4623E-03	1.3816E+00	.2266
2.96	8.2000	.0434	21.580	1.680	27.83	3.000	547	187	2121.29	1.5342	3.7287E-03	3.1470E-03	1.5294E+00	.2883
3.80	8.2000	.0300	23.000	1.699	28.19	3.196	547	180	2129.91	1.6321	2.7069E-03	2.1475E-03	1.6286E+00	.3338
4.93	8.2000	.0141	24.800	1.699	28.62	3.323	548	171	2141.30	1.7591	1.3432E-03	9.4993E-04	1.7534E+00	.4021
6.19	8.2000	.0044	26.400	1.686	28.88	3.435	548	163	2153.83	1.8614	4.3992E-04	3.0603E-04	1.8608E+00	.4719
7.46	8.2000	0.0000	27.550	1.680	29.00	3.518	5.8	158	2164.73	1.9354	0.	0.	1.9354E+00	.5291

TABLE I.- TABULATED DATA - Continued

Test 3 SURVEY 3-1-120V

QJ/QI = 1.0063 LAMDA = .5689

JET GAS	MOL.WT.	SPECIFIC HEAT	GAMMA	AVG.TOTAL TEMP.(DEG.R)	TOTAL PRESS.(PSIA)
TUNNEL GAS	2.015	3.4160	1.405	541	39.32
	29.000	.2400	1.399	541	200.84

RHOVJ = 1.0630E+00 XIM = 1.6337E-02 GXM = 2.7061E-02 AIRMEN = 1.8666E+00 AKXM = 2.8577E-01

Y/D	Z/D	K	PT2x	P1X	MWX	MX	TYX	TX	VX	RHOVX	XI	GX	RHOVX*(1-GX)	PRM
COORDINATES	MOL FR.	PSIA	PSIA	MOL WT	MACH	-DEG.R.-	FT/SEC	SLG/SQFTSEC	MASS FR.	AIR MASS FLOW				
0.00	.2250	.2002	4.007	1.330	23.38	1.407	541	387	1510.57	.3513	5.9303E-03	1.7946E-02	3.4497E-01	.0213
0.00	1.4750	.2609	6.936	1.330	21.96	1.895	541	315	1892.18	.5089	1.1464E-02	2.3947E-02	4.9671E-01	.0440
0.00	2.2250	.2778	9.659	1.325	21.50	2.299	541	263	2120.04	.6662	1.6320E-02	2.6039E-02	6.4887E-01	.0823
0.00	2.7250	.2838	8.367	1.325	21.34	2.127	541	284	2046.24	.5910	1.4902E-02	2.6803E-02	5.7516E-01	.0629
0.00	3.2250	.2858	8.791	1.300	21.29	2.208	541	274	2088.42	.6120	1.5580E-02	2.7061E-02	5.9541E-01	.0700
0.00	3.6750	.2788	9.563	1.360	21.48	2.255	541	268	2101.30	.6637	1.6337E-02	2.6165E-02	6.4632E-01	.0789
0.00	5.2250	.2207	11.730	1.365	23.04	2.516	541	239	2135.61	.8158	1.4419E-02	1.9308E-02	8.0007E-01	.1196
0.00	6.2250	.1239	15.038	1.378	25.49	2.847	541	206	2135.86	1.0540	1.0198E-02	1.0275E-02	1.0431E+00	.2001
0.00	7.2250	.0479	20.647	1.355	27.71	3.490	541	164	2176.17	1.4425	4.7244E-03	3.4015E-03	1.4375E+00	.4402
0.00	8.2250	.0396	25.555	1.345	28.77	3.795	541	140	2204.62	1.7707	1.3045E-03	6.0301E-04	1.7697E+00	.7771
0.00	9.2250	0.0000	26.972	1.355	29.00	3.886	541	135	2209.06	1.8666	0.	0.	1.8666E+00	.8805
-0.00	3.2250	.2858	8.781	.280	21.29	4.897	546	94	2716.44	.4987	1.2768E-02	2.7061E-02	4.8521E-01	.6535
-11.29	3.2250	0.0000	17.131	1.175	29.00	3.308	546	171	2121.09	1.2214	0.	0.	1.2214E+00	.3398
-10.69	3.2250	.0309	17.063	1.180	28.98	3.297	546	172	2119.70	1.2192	6.8901E-05	5.9736E-05	1.2191E+00	.3358
-9.29	3.2250	.0317	16.928	1.225	28.95	3.220	546	178	2104.64	1.2163	1.3761E-04	1.1960E-04	1.2161E+00	.3317
-6.96	3.2250	.0069	18.084	1.285	28.81	3.251	546	176	2116.16	1.2911	5.8092E-04	4.8140E-04	1.2925E+00	.3419
-5.06	3.2250	.0233	18.856	1.470	28.37	3.098	546	187	2090.79	1.3548	2.1248E-03	1.6578E-03	1.3525E+00	.3322
-3.71	3.2250	.0700	16.945	1.405	27.11	3.004	546	195	2123.77	1.2031	5.9278E-03	5.2078E-03	1.1949E+00	.2592
-2.70	3.2250	.1373	12.281	1.365	25.29	2.572	546	235	2069.41	.8803	9.1152E-03	1.0945E-02	8.7062E-01	.1362
-1.69	3.2250	.2120	11.334	1.370	23.28	2.467	546	246	2116.55	.7943	1.3797E-02	1.8360E-02	7.7974E-01	.1110
-1.67	3.2250	.2738	9.293	1.400	21.61	2.186	546	272	2072.34	.6509	1.6726E-02	2.5537E-02	6.3429E-01	.0711
-0.00	3.2250	.2358	8.781	1.280	21.29	2.225	546	274	2104.94	.6066	1.5530E-02	2.7061E-02	5.9318E-01	.0710
.94	3.2250	.2638	9.640	1.295	21.88	2.325	546	262	2123.63	.6648	1.5248E-02	2.4308E-02	6.4862E-01	.0840
1.62	3.2250	.2091	11.628	1.380	23.36	2.484	546	244	2119.54	.8100	1.3832E-02	1.8049E-02	7.9540E-01	.1148
2.97	3.2250	.1097	15.366	1.530	28.04	2.726	546	220	2088.57	1.0973	8.4211E-03	8.4970E-03	1.0880E+00	.1851
3.84	3.2250	.0576	17.776	1.435	27.45	3.042	546	192	2120.29	1.2625	5.0514E-03	4.2292E-03	1.2572E+00	.2804
6.07	3.2250	.0386	19.538	1.382	28.77	3.263	546	175	2120.37	1.3982	7.9767E-04	6.0301E-04	1.3976E+00	.3742
7.61	3.2250	.0034	19.048	1.340	28.91	3.268	546	174	2116.29	1.3624	3.0895E-04	2.3969E-04	1.3621E+00	.3655
8.75	3.2250	.0017	18.239	1.325	28.95	3.214	546	178	2103.26	1.3111	1.4815E-04	1.1960E-04	1.3110E+00	.3340
9.82	3.2250	.0009	17.429	1.315	28.98	3.151	546	183	2088.81	1.2598	7.1195E-05	5.9736E-05	1.2597E+00	.3023
11.29	3.2250	0.0000	17.487	1.265	29.00	3.221	546	178	2133.09	1.2574	0.	0.	1.2574E+00	.3222

TABLE I.- TABULATED DATA - Continued

Test 3 - Concluded

Y/O	Z/O	K	PT2K	P1X	MWX	MX	YTX	TX	VX	RHOVX	X1	GX	RHOVX*(1-SX)	PRM
COORDINATES		MOL FR.	PSIA	PSIA	MOL WT	MACH	-DEG.R.-		FT/SEC	SLG/SQFTSEC		MASS FR.	AIR MASS FLOW	
-0.00	1.7250	.2678	7.307	1.325	21.77	1.975	.543	305	1950.37	.5344	1.2479E-02	2.4795E-02	5.2119E-01	.0498
-13.36	1.7250	0.0000	10.594	1.230	29.00	2.513	.544	241	1938.84	.8197	0.	0.	8.1973E-01	.1070
-12.03	1.7250	.6917	10.353	1.260	20.95	2.452	.544	247	1999.44	.8077	9.0962E-05	1.1960E-04	0.0761E-01	.0997
-11.16	1.7250	.0034	10.449	1.278	28.91	2.445	.544	248	1988.67	.8153	1.8491E-04	2.3969E-04	8.1907E-01	.1001
-9.22	1.7250	.0077	10.257	1.318	28.79	2.382	.544	255	1959.53	.8058	4.1137E-04	5.4214E-04	8.0536E-01	.0935
-7.54	1.7250	.0190	10.546	1.355	28.49	2.387	.544	255	1879.42	.8242	1.0427E-03	1.3436E-03	8.2306E-01	.0961
-5.39	1.7250	.0452	11.664	1.350	27.78	2.508	.544	241	1948.40	.8049	2.7337E-03	3.2807E-03	8.8199E-01	.1175
-3.04	1.7250	.1272	11.626	1.300	25.57	2.564	.544	235	2049.98	.8405	7.9359E-03	1.0027E-02	8.3207E-01	.1225
-2.67	1.7250	.2480	8.020	1.350	22.31	2.057	.544	294	1971.04	.5868	1.2344E-02	2.2416E-02	5.7167E-01	.0577
-0.00	1.7250	.2678	7.307	1.320	21.77	1.979	.543	304	1952.65	.5340	1.2469E-02	2.4795E-02	5.2079E-01	.0499
1.55	1.7250	.1900	10.141	1.310	23.87	2.374	.544	255	2048.71	.7269	1.0979E-02	1.6040E-02	7.1521E-01	.0918
3.37	1.7250	.0988	12.030	1.412	26.33	2.499	.544	242	1997.61	.8899	6.3400E-03	7.5661E-03	8.8313E-01	.1203
5.34	1.7250	.0917	11.780	1.390	27.88	2.492	.544	243	1939.63	.8971	2.5469E-03	3.0151E-03	8.9436E-01	.1171
6.87	1.7250	.0199	11.433	1.360	28.46	2.482	.544	244	1915.95	.8809	1.1665E-03	1.4062E-03	8.7969E-01	.1127
8.89	1.7250	.0086	10.739	1.332	28.77	2.427	.544	250	1886.75	.8380	4.7583E-04	6.0301E-04	8.3748E-01	.1016
10.69	1.7250	.0034	10.488	1.305	28.91	2.421	.544	250	1880.77	.8208	1.8526E-04	2.3969E-04	8.2062E-01	.0987
12.16	1.7250	.0017	10.816	1.285	28.95	2.483	.544	244	1900.41	.8403	9.4628E-05	1.1960E-04	8.4016E-01	.1068
13.36	1.7250	0.0000	10.237	1.260	29.00	2.429	.544	250	1879.88	.8018	0.	0.	8.0179E-01	.0968
-0.00	1.1000	.1299	15.115	1.360	25.49	2.875	.546	206	2154.93	1.0514	1.0221E-02	1.0275E-02	1.0406E+00	.2064
-6.40	1.1000	0.0000	26.992	1.210	29.00	4.119	.546	124	2250.29	1.8386	0.	0.	1.8386E+00	1.0759
-5.39	1.1000	.0009	26.490	1.230	28.94	4.046	.546	128	2241.86	1.8098	1.0228E-04	5.9736E-05	1.8096E+00	.9927
-4.25	1.1000	.0121	25.199	1.277	28.67	3.869	.546	137	2229.25	1.7277	1.3858E-03	8.4779E-04	1.7263E+00	.8124
-3.26	1.1000	.0312	22.789	1.305	28.16	3.634	.546	150	2212.70	1.5692	3.3133E-03	2.2319E-03	1.5656E+00	.6007
-2.56	1.1000	.0549	20.321	1.332	27.52	3.399	.546	166	2193.61	1.4057	5.3506E-03	4.0235E-03	1.4000E+00	.4330
-1.82	1.1000	.0844	17.814	1.349	26.72	3.146	.546	183	2173.60	1.2374	7.4511E-03	6.3651E-03	1.2295E+00	.3074
-1.21	1.1000	.1070	16.291	1.350	26.11	3.001	.546	195	2163.09	1.1330	8.4555E-03	8.2618E-03	1.1236E+00	.2479
-0.67	1.1000	.1226	15.385	1.360	25.69	2.901	.546	204	2153.37	1.0715	9.7491E-03	9.6174E-03	1.0612E+00	.2149
-0.00	1.1000	.1299	15.115	1.360	25.49	2.875	.546	206	2154.93	1.0514	1.0221E-02	1.0275E-02	1.0406E+00	.2064
.08	1.1000	.1152	15.366	1.355	25.99	2.905	.546	203	2146.77	1.0739	9.1156E-03	8.9725E-03	1.0642E+00	.2154
1.42	1.1000	.0925	17.159	1.350	26.50	3.083	.546	188	2167.56	1.1934	7.9428E-03	7.0352E-03	1.1850E+00	.2803
2.23	1.1000	.0629	19.569	1.345	27.30	3.307	.546	171	2185.61	1.3565	5.9607E-03	4.6448E-03	1.3502E+00	.3883
3.04	1.1000	.0387	22.075	1.337	27.97	3.530	.546	156	2202.22	1.5248	3.9694E-03	2.7517E-03	1.5206E+00	.5317
3.91	1.1000	.0173	24.736	1.325	28.53	3.760	.546	143	2218.48	1.7018	1.9624E-03	1.2189E-03	1.6998E+00	.7268
4.99	1.1000	.0043	26.490	1.325	28.88	3.895	.546	136	2224.91	1.8204	5.1653E-04	2.9993E-04	1.8198E+00	.8733
6.07	1.1000	0.0000	27.127	1.322	29.00	3.947	.546	133	2227.17	1.8629	0.	0.	1.8629E+00	.9350

TABLE I.- TABULATED DATA - Continued

Test 4 SURVEY 3-1-120V

1.C051 LAMDA = .5689

	MOL.WT.	SPECIFIC HEAT	GAMMA	AVG.TOTAL TEMP.(IDFG.R)	TOTAL PRESS.(PSIA)
JET GAS	2.016	3.4100	1.406	529	39.09
TUNNEL GAS	29.000	.2400	1.399	530	199.91

RHOVJ = 1.C650E+00 XFM = 1.5644E-02 GXM = 2.3554E-02 AIRMFH = 1.9312E+00 AKXM = 2.5761E-01

Y/D	Z/D	K	PT2X	P1X	PMX	MX	TTX	TX	VX	RHOVX	XT	GX	RHOVX*11-GX1	PRM
COORDINATES	MOL FR.	PSIA	PSIA	MOL WT	MACH	-DEG.R.-	FT/SEC	SLG/SQFTSEC	MASS FR.	AIR MASS FLOW				
0.00	.6000	.1837	4.158	1.369	24.04	1.402	530	380	1470.88	.3666	5.2819E-03	1.5403E-02	3.6092E-01	.0217
0.00	1.1000	.2019	6.990	1.372	23.55	1.890	530	309	1805.64	.5474	8.8502E-03	1.7283E-02	5.3795E-01	.0453
0.00	1.6000	.2182	8.382	1.372	23.11	2.089	530	283	1927.57	.6266	1.1159E-02	1.9027E-02	6.1468E-01	.0617
0.00	2.1000	.2347	8.766	1.375	22.67	2.138	530	276	1970.27	.6436	1.2569E-02	2.0876E-02	6.3016E-01	.0668
0.00	2.6000	.2482	9.294	1.352	22.33	2.227	530	266	2028.12	.6671	1.4002E-02	2.2436E-02	6.5214E-01	.0755
0.00	3.1000	.2566	9.582	1.342	22.08	2.273	530	260	2059.18	.6794	1.4891E-02	2.3428E-02	6.6351E-01	.0805
0.00	3.6000	.2655	10.014	1.342	22.11	2.328	530	254	2081.64	.7047	1.5361E-02	2.3303E-02	6.8825E-01	.0876
0.00	4.1000	.2742	10.734	1.347	22.33	2.418	530	244	2108.43	.7494	1.5644E-02	2.2714E-02	7.5271E-01	.1007
0.00	4.6500	.2844	11.742	1.349	22.94	2.531	530	232	2123.40	.8185	1.5096E-02	1.9716E-02	8.0234E-01	.1206
0.00	5.1000	.2938	12.942	1.352	23.77	2.657	530	219	2130.19	.9040	1.3899E-02	1.6435E-02	8.8913E-01	.1474
0.00	5.6500	.2978	14.814	1.360	25.01	2.844	530	202	2133.96	1.0396	1.1587E-02	1.1914E-02	1.0273E+00	.1975
0.00	6.1000	.2978	17.022	1.357	26.09	3.062	530	184	2146.59	1.1948	9.3083E-03	8.3278E-03	1.1849E+00	.2735
0.00	6.6000	.2996	19.230	1.342	27.12	3.281	530	168	2154.65	1.3514	6.5358E-03	5.1697E-03	1.3445E+00	.3737
0.00	7.1000	.3049	22.590	1.322	28.06	3.593	530	148	2176.97	1.5800	3.7066E-03	2.5077E-03	1.5761E+00	.5757
0.00	7.6000	.3164	25.422	1.315	28.56	3.828	530	135	2194.93	1.7694	1.9219E-03	1.1611E-03	1.7673E+00	.7434
0.00	8.1000	.3046	27.006	1.307	28.88	3.961	530	128	2201.39	1.8771	5.5820E-04	3.1788E-04	1.8765E+00	.9439
0.00	8.6500	1.0000	27.822	1.300	29.00	4.033	530	125	2206.22	1.9312	0.	0.	1.9312E+00	1.0335
0.00	9.2500	.2420	9.294	1.365	22.47	2.216	530	267	2015.31	.6708	1.3623E-02	2.1709E-02	6.5676E-01	.0748
0.00	9.8500	.2576	9.390	1.342	22.05	2.249	530	263	2049.43	.6679	1.4717E-02	2.3554E-02	6.5220E-01	.0774
0.00	1.3500	.2576	9.774	1.342	22.05	2.297	530	257	2071.23	.6900	1.5204E-02	2.3554E-02	6.7375E-01	.0836
0.00	1.8500	.2534	10.266	1.341	22.16	2.252	530	251	2089.52	.7165	1.5452E-02	2.3053E-02	6.9997E-01	.0910
8.95	3.1000	0.0000	18.462	1.345	29.00	3.209	533	174	2075.42	1.3448	0.	0.	1.3448E+00	.3357
7.61	3.1000	.0019	18.702	1.345	28.95	3.231	533	173	2081.74	1.3588	1.6533E-04	1.3023E-04	1.3586E+00	.3465
6.13	3.1000	.0037	19.662	1.340	28.90	3.322	533	166	2102.06	1.4174	3.4571E-04	2.6106E-04	1.4170E+00	.3943
5.46	3.1000	.0056	20.286	1.335	28.85	3.382	533	162	2115.63	1.4547	5.3343E-04	3.9248E-04	1.4541E+00	.4288
4.72	3.1000	.0131	20.718	1.337	28.65	3.417	533	160	2129.47	1.4770	1.2754E-03	9.2423E-04	1.4756E+00	.4511
4.18	3.1000	.0226	20.718	1.338	28.39	3.415	533	160	2138.60	1.4707	2.2024E-03	1.6029E-03	1.4683E+00	.4505
3.37	3.1000	.0493	19.470	1.342	27.67	3.302	533	168	2143.53	1.3760	4.6152E-03	3.5901E-03	1.3710E+00	.3836
2.77	3.1000	.0764	16.574	1.342	26.94	3.075	533	184	2121.57	1.2059	6.4400E-03	5.7160E-03	1.1990E+00	.2746
2.02	3.1000	.1419	13.758	1.342	25.17	2.755	532	211	2106.21	.9754	1.0359E-02	1.1368E-02	9.6427E-01	.1693
1.35	3.1000	.1974	11.022	1.342	23.67	2.450	532	242	2065.30	.7869	1.2355E-02	1.6805E-02	7.7363E-01	.1056
.67	3.1000	.2416	9.102	1.342	22.48	2.211	532	269	2017.10	.6562	1.3285E-02	2.1669E-02	6.4196E-01	.0727
-0.00	3.1000	.2631	8.574	1.342	21.90	2.141	532	277	2009.62	.6173	1.3967E-02	2.4217E-02	6.0236E-01	.0651
-.67	3.1000	.2545	9.150	1.342	22.13	2.217	532	268	2035.58	.6539	1.4162E-02	2.3179E-02	6.3878E-01	.0774
-1.42	3.1000	.2099	11.166	1.338	23.34	2.471	532	239	2088.05	.7893	1.3371E-02	1.8133E-02	7.7496E-01	.1088
-2.02	3.1000	.1684	13.086	1.338	24.46	2.688	532	218	2115.15	.9216	1.1953E-02	1.3882E-02	9.0879E-01	.1521
-2.63	3.1000	.1178	15.246	1.333	25.82	2.918	533	197	2126.08	1.0763	9.2502E-03	9.1988E-03	1.0664E+00	.2154
-3.37	3.1000	.0744	16.830	1.320	26.99	3.088	533	183	2122.08	1.1955	6.2052E-03	5.5593E-03	1.1888E+00	.2754
-4.05	3.1000	.0416	17.838	1.320	27.88	3.183	533	176	2110.50	1.2771	3.5900E-03	3.0087E-03	1.2733E+00	.3169
-4.72	3.1000	.0264	18.126	1.320	28.29	3.210	533	174	2101.08	1.3043	2.2855E-03	1.8788E-03	1.3018E+00	.3296
-5.39	3.1000	.0160	18.078	1.320	28.57	3.205	533	175	2089.95	1.3076	1.3758E-03	1.1262E-03	1.3061E+00	.3276
-6.07	3.1000	.0094	17.694	1.325	28.75	3.164	533	178	2074.58	1.2881	7.9084E-04	6.5713E-04	1.2872E+00	.3093
-6.74	3.1000	.0056	17.430	1.325	28.85	3.139	533	180	2065.59	1.2737	4.6705E-04	3.9248E-04	1.2732E+00	.2902
-7.48	3.1000	.0047	17.070	1.325	28.87	3.105	533	182	2057.12	1.2515	3.8199E-04	3.2669E-04	1.2511E+00	.2836
-8.15	3.1000	.0028	16.638	1.327	28.92	3.062	533	186	2045.36	1.2255	2.2393E-04	1.9557E-04	1.2253E+00	.2663
-8.75	3.1000	0.0000	16.302	1.327	29.00	3.029	533	188	2035.14	1.2058	0.	0.	1.2058E+00	.2537
-9.42	3.1000	0.0000	16.206	1.327	29.00	3.020	533	189	2032.93	1.1997	0.	0.	1.1997E+00	.2507

TABLE I.- TABULATED DATA - Continued

Test 4 - Concluded

Y/O	Z/O	K	PT2X	PIX	MWX	HX	TYX	Y	VX	RHOVX	KI	GX	RHOVX*(1-GX)	PRH
COORDINATES		MOL FR.	PSIA	PSIA	MOL WT	MACH	-DEG.	R.-	FT/SEC	SLG/SOFTSEC		MASS FR.	AIR MASS FLOW	
13.49	1.6000	0.0000	10.550	1.365	29.00	2.421	534	246	1859.60	.0666	0.	0.	8.6662E-01	.1023
12.83	1.6000	.0018	10.054	1.365	28.95	2.409	534	247	1857.07	.8597	9.8577E-05	1.2285E-04	8.5958E-01	.1005
12.16	1.6000	.0018	10.806	1.365	28.95	2.404	534	248	1855.03	.8566	9.8219E-05	1.2285E-04	8.5646E-01	.0996
11.43	1.6000	.0018	11.710	1.365	28.95	2.392	534	249	1850.92	.8503	9.7503E-05	1.2285E-04	8.5022E-01	.0979
10.76	1.6000	.0018	10.494	1.365	28.95	2.366	534	252	1841.48	.8363	9.5891E-05	1.2285E-04	8.3616E-01	.0940
10.09	1.6000	.0035	10.230	1.365	28.90	2.334	534	256	1831.04	.8184	1.8808E-04	2.4623E-04	8.1818E-01	.0894
9.42	1.6000	.0062	10.062	1.365	28.83	2.313	534	258	1825.45	.8064	3.2539E-04	4.3229E-04	8.0609E-01	.0866
8.68	1.6000	.0097	10.062	1.367	28.74	2.312	534	258	1827.73	.8053	5.1285E-04	6.8226E-04	8.0480E-01	.0864
7.75	1.6000	.0142	10.158	1.367	28.62	2.323	534	257	1836.00	.8099	7.5430E-04	9.9777E-04	8.0913E-01	.0880
6.81	1.6000	.0213	10.782	1.374	28.43	2.392	534	249	1867.74	.8404	1.1955E-03	1.5050E-03	8.4708E-01	.0985
5.80	1.6000	.0302	11.558	1.372	28.18	2.499	534	239	1909.85	.8968	1.8103E-03	2.1626E-03	8.9489E-01	.1144
4.72	1.6000	.0446	12.462	1.368	27.80	2.589	534	228	1956.53	.9449	2.8557E-03	3.2379E-03	9.4185E-01	.1334
3.71	1.6000	.0674	12.678	1.369	27.18	2.613	534	226	1985.75	.9481	4.4230E-03	4.4581E-03	9.4336E-01	.1303
2.70	1.6000	.1100	11.958	1.372	26.03	2.529	533	234	2000.18	.8847	7.0348E-03	8.5154E-03	8.7713E-01	.1218
1.62	1.6000	.1662	9.966	1.375	24.52	2.292	533	260	1968.29	.7400	9.4380E-03	1.3664E-02	7.2989E-01	.0843
.61	1.6000	.2311	7.422	1.375	22.76	1.952	523	302	1875.69	.5632	1.0758E-02	2.0464E-02	5.5167E-01	.0496
-0.00	1.6000	.2502	7.134	1.375	22.25	1.909	533	308	1873.29	.5397	1.1420E-02	2.2671E-02	5.2744E-01	.0464
-1.01	1.6000	.2052	8.502	1.380	23.46	2.099	533	283	1923.25	.6375	1.0494E-02	1.7636E-02	6.2626E-01	.0625
-1.96	1.6000	.1517	9.918	1.375	24.91	2.206	533	261	1950.59	.7428	8.5154E-03	1.2282E-02	7.3371E-01	.0835
-2.97	1.6000	.1007	10.638	1.370	26.28	2.378	533	250	1935.91	.8071	5.8157E-03	7.7205E-03	8.0082E-01	.0962
-4.05	1.6000	.0573	10.662	1.358	27.45	2.393	534	249	1900.20	.8247	3.2414E-03	4.2111E-03	8.2118E-01	.0975
-5.06	1.6000	.0338	10.158	1.350	28.09	2.339	534	255	1858.92	.8007	1.8145E-03	2.4279E-03	7.9876E-01	.0891
-6.13	1.6000	.0177	9.774	1.355	28.52	2.287	534	261	1824.84	.7824	9.1475E-04	1.2527E-03	7.8138E-01	.0824
-7.67	1.6000	.0088	9.630	1.357	28.76	2.267	534	264	1809.56	.7764	4.4899E-04	5.1956E-04	7.7594E-01	.0800
-8.15	1.6000	.0035	9.390	1.360	28.90	2.233	534	268	1791.91	.7629	1.7533E-04	2.4623E-04	7.6269E-01	.0761
-8.82	1.6000	.0018	9.438	1.362	28.95	2.238	534	267	1792.22	.7669	8.7933E-05	1.2285E-04	7.6677E-01	.0767
-9.22	1.6000	0.0000	9.678	1.362	29.00	2.268	534	263	1802.65	.7833	0.	0.	7.8326E-01	.0805
5.39	5.8500	0.0000	27.774	1.320	29.00	3.998	534	127	2209.97	1.9238	0.	0.	1.9238E+00	.9953
4.65	5.8500	.0009	27.534	1.325	28.98	3.973	534	129	2207.49	1.9088	1.0955E-04	6.1429E-05	1.9087E+00	.9656
4.05	5.8500	.0053	27.102	1.335	28.86	3.926	534	131	2205.54	1.8795	6.5070E-04	3.7056E-04	1.8788E+00	.9131
3.31	5.8500	.0177	25.662	1.360	28.52	3.781	534	139	2197.35	1.7830	2.0892E-03	1.2541E-03	1.7808E+00	.7641
2.70	5.8500	.0330	23.466	1.367	28.11	3.597	534	149	2183.52	1.6323	3.6054E-03	2.3641E-03	1.6284E+00	.5546
1.96	5.8500	.0620	19.998	1.365	27.33	3.319	534	167	2162.04	1.4017	5.9873E-03	4.5719E-03	1.3953E+00	.3991
1.21	5.8500	.0915	16.574	1.360	26.53	3.054	534	186	2136.22	1.1981	7.7792E-03	6.9455E-03	1.1898E+00	.2492
.61	5.8500	.1186	15.246	1.360	25.80	2.888	533	200	2120.41	1.0782	9.3359E-03	9.2677E-03	1.0682E+00	.2095
-.13	5.8500	.1404	14.166	1.360	25.21	2.778	533	210	2113.19	1.0018	1.0510E-02	1.1229E-02	9.9051E-01	.1775
-.81	5.8500	.1623	14.266	1.360	25.16	2.791	533	208	2118.99	1.0079	1.0740E-02	1.1405E-02	9.9641E-01	.1808
-1.55	5.8500	.1214	15.534	1.352	25.72	2.525	523	197	2133.68	1.0929	9.7183E-03	9.5171E-03	1.0825E+00	.2204
-2.29	5.8500	.0915	17.838	1.312	26.53	3.193	534	176	2166.62	1.2444	8.0796E-03	6.9455E-03	1.2357E+00	.3190
-3.10	5.8500	.0556	21.158	1.282	27.50	3.533	534	153	2196.01	1.4684	5.5909E-03	4.0751E-03	1.4624E+00	.5093
-3.98	5.8500	.0267	24.542	1.280	28.28	3.844	534	135	2215.81	1.7199	3.0564E-03	1.9020E-03	1.7167E+00	.7835
-4.65	5.8500	.0115	26.670	1.278	28.69	3.981	534	128	2219.43	1.8392	1.3901E-03	8.0858E-04	1.8377E+00	.9419
-5.60	5.8500	.0018	27.566	1.278	28.55	4.079	534	124	2222.20	1.9282	2.2157E-04	1.2299E-04	1.9279E+00	1.0729
-6.07	5.8500	0.0000	28.302	1.280	29.00	4.101	534	123	2223.13	1.9510	0.	0.	1.9510E+00	1.1059
-6.67	5.8500	0.0000	28.734	1.278	29.00	4.136	534	121	2227.46	1.9776	0.	0.	1.9776E+00	1.1563

TABLE I.- TABULATED DATA - Continued

Test 5 SURVEY 35 9590,,239

CJ/QI = 1.0012 LAMDA = .5772

	MCL.WT.	SPECIFIC HEAT	GAMMA	AVG.TOTAL TEMP.(DEG.R)	TOTAL PRESS.(PSIA)
JET GAS	2.016	3.4300	1.403	505	48.65
TUNNEL GAS	29.000	.2400	1.259	530	249.75

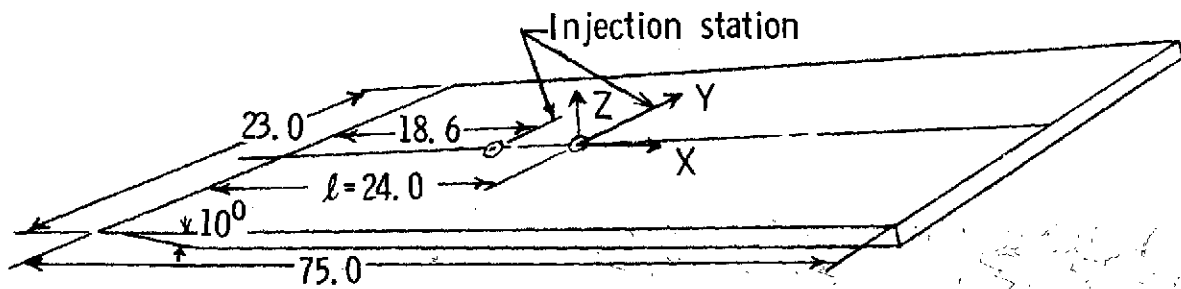
PHOVJ • 1.3552F+CO

Y/D	Z/D	K	PTX	PTX	MX	MX	TX	TX	VX	ROCVX	XI	GX	ROCVX(1-GX)	PRM
(COORD)	(DATE)	(MID PT)	(PTA)	(PTA)	(MID WT)	(MAG)	(-NEG.)	(-NEG.)	(PTA/C)	(SIG/SEC)	(SEC)	(MAX PT)	(ATN MAX PT)	(PRM)
0.00	1.0000	2.001	1.000	1.000	2.000	1.000	526	427	1209.81	1.434	4.2940E-01	1.7311E-01	1.2449E-01	0.0144
0.00	1.0100	2.001	1.000	1.000	2.000	1.000	526	427	1209.81	1.434	4.2940E-01	1.7311E-01	1.2449E-01	0.0144
0.00	1.0200	2.001	1.000	1.000	2.000	1.000	526	427	1209.81	1.434	4.2940E-01	1.7311E-01	1.2449E-01	0.0144
0.00	1.0300	2.001	1.000	1.000	2.000	1.000	526	427	1209.81	1.434	4.2940E-01	1.7311E-01	1.2449E-01	0.0144
0.00	1.0400	2.001	1.000	1.000	2.000	1.000	526	427	1209.81	1.434	4.2940E-01	1.7311E-01	1.2449E-01	0.0144
0.00	1.0500	2.001	1.000	1.000	2.000	1.000	526	427	1209.81	1.434	4.2940E-01	1.7311E-01	1.2449E-01	0.0144
0.00	1.0600	2.001	1.000	1.000	2.000	1.000	526	427	1209.81	1.434	4.2940E-01	1.7311E-01	1.2449E-01	0.0144
0.00	1.0700	2.001	1.000	1.000	2.000	1.000	526	427	1209.81	1.434	4.2940E-01	1.7311E-01	1.2449E-01	0.0144
0.00	1.0800	2.001	1.000	1.000	2.000	1.000	526	427	1209.81	1.434	4.2940E-01	1.7311E-01	1.2449E-01	0.0144
0.00	1.0900	2.001	1.000	1.000	2.000	1.000	526	427	1209.81	1.434	4.2940E-01	1.7311E-01	1.2449E-01	0.0144
0.00	1.1000	2.001	1.000	1.000	2.000	1.000	526	427	1209.81	1.434	4.2940E-01	1.7311E-01	1.2449E-01	0.0144
0.00	1.1100	2.001	1.000	1.000	2.000	1.000	526	427	1209.81	1.434	4.2940E-01	1.7311E-01	1.2449E-01	0.0144
0.00	1.1200	2.001	1.000	1.000	2.000	1.000	526	427	1209.81	1.434	4.2940E-01	1.7311E-01	1.2449E-01	0.0144
0.00	1.1300	2.001	1.000	1.000	2.000	1.000	526	427	1209.81	1.434	4.2940E-01	1.7311E-01	1.2449E-01	0.0144
0.00	1.1400	2.001	1.000	1.000	2.000	1.000	526	427	1209.81	1.434	4.2940E-01	1.7311E-01	1.2449E-01	0.0144
0.00	1.1500	2.001	1.000	1.000	2.000	1.000	526	427	1209.81	1.434	4.2940E-01	1.7311E-01	1.2449E-01	0.0144
0.00	1.1600	2.001	1.000	1.000	2.000	1.000	526	427	1209.81	1.434	4.2940E-01	1.7311E-01	1.2449E-01	0.0144
0.00	1.1700	2.001	1.000	1.000	2.000	1.000	526	427	1209.81	1.434	4.2940E-01	1.7311E-01	1.2449E-01	0.0144
0.00	1.1800	2.001	1.000	1.000	2.000	1.000	526	427	1209.81	1.434	4.2940E-01	1.7311E-01	1.2449E-01	0.0144
0.00	1.1900	2.001	1.000	1.000	2.000	1.000	526	427	1209.81	1.434	4.2940E-01	1.7311E-01	1.2449E-01	0.0144
0.00	1.2000	2.001	1.000	1.000	2.000	1.000	526	427	1209.81	1.434	4.2940E-01	1.7311E-01	1.2449E-01	0.0144
0.00	1.2100	2.001	1.000	1.000	2.000	1.000	526	427	1209.81	1.434	4.2940E-01	1.7311E-01	1.2449E-01	0.0144
0.00	1.2200	2.001	1.000	1.000	2.000	1.000	526	427	1209.81	1.434	4.2940E-01	1.7311E-01		

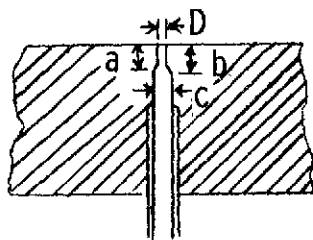
TABLE I.- TABULATED DATA - Concluded

Test 5 - Concluded

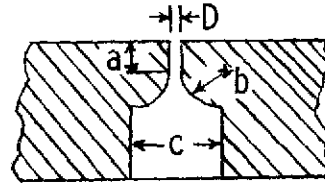
Y/D COORDINATES	Z/D	K MDL FR.	P72X PSIA	P1X PSIA	MWR MOL WT	MX MACH	TYX -DEG.R.-	TY	VX FT/SEC	RHOVX SLG/SOFTSEC	RT	GK MASS FR.	RHOVX*(1-GK) AIR MASS FLOW	PRM
4.50	2.2474	.2040	15.500	1.713	22.14	2.580	528	225	2003.11	1.1475	6.9202E-03	8.1725E-03	1.1381E+00	.1327
5.12	2.2474	.0602	16.900	1.709	27.92	2.704	529	215	1979.51	1.2722	2.7258E-03	2.9034E-03	1.2685E+00	.1604
7.52	2.2474	.0172	16.800	1.690	26.54	2.686	530	211	1953.49	1.2570	1.1259E-03	1.2174E-03	1.2563E+00	.1543
9.19	2.2474	.0098	15.050	1.680	28.74	2.567	530	229	1910.08	1.1677	5.9058E-04	6.8540E-04	1.1669E+00	.1275
9.92	2.2474	.0086	14.080	1.680	26.77	2.470	530	231	1879.58	1.1057	4.9140E-04	4.0228E-04	1.1050E+00	.1110
10.70	2.2474	.0060	13.400	1.673	28.84	2.419	530	240	1855.86	1.0620	3.2935E-04	4.2027E-04	1.0615E+00	.1008
11.40	2.2474	.0034	13.400	1.665	28.91	2.425	530	240	1856.94	1.0623	1.8766E-04	2.3940E-04	1.0620E+00	.1013
12.25	2.2474	.0017	13.550	1.660	28.95	2.481	530	238	1875.02	1.0583	5.6810E-05	1.1545E-04	1.0582E+00	.1103
-6.36	3.8569	.0009	25.900	1.568	28.98	3.531	530	152	2121.97	1.8479	8.1354E-05	5.9664E-05	1.8477E+00	.5011
-4.73	3.8569	.0034	27.300	1.585	28.91	3.608	530	147	2147.43	1.9361	3.4203E-04	2.3940E-04	1.9356E+00	.5644
-3.26	3.8569	.0227	25.880	1.610	28.35	3.482	530	155	2144.25	1.8343	2.1869E-03	1.6156E-03	1.8314E+00	.4797
-1.71	3.8569	.0403	20.050	1.658	26.56	3.004	528	180	2110.17	1.4294	7.2311E-03	6.8554E-03	1.4196E+00	.2456
0.00	3.8569	.2150	13.700	1.770	22.20	2.411	526	243	2053.23	.9753	1.3500E-02	1.8682E-02	5.6101E-01	.1024
.62	3.8569	.2495	12.230	1.735	22.27	2.258	525	260	2034.50	.8767	1.4614E-02	2.2589E-02	8.5650E-01	.0813
1.40	3.8569	.2675	11.450	1.733	21.78	2.180	524	269	2020.29	.8223	1.5019E-02	2.4753E-02	8.0151E-01	.0720
2.17	3.8569	.2621	11.730	1.740	21.92	2.204	525	266	2025.01	.8418	1.4565E-02	2.4051E-02	8.2152E-01	.0750
4.07	3.8569	.2335	12.530	1.740	22.70	2.323	525	255	2043.81	.9263	1.4174E-02	2.0737E-02	9.0706E-01	.0603
4.65	3.8569	.1155	19.000	1.740	25.87	2.848	528	201	2045.34	1.3580	9.0516E-03	5.0326E-03	1.3457E+00	.2016
6.12	3.8569	.0235	26.530	1.713	28.36	3.416	530	159	2132.90	1.8882	2.3311E-03	1.6730E-03	1.8851E+00	.4643
7.60	3.8569	.0026	28.000	1.660	28.93	3.569	530	150	2140.15	1.9913	2.6356E-04	1.7936E-04	1.9909E+00	.5555
9.15	3.8569	.0017	25.550	1.638	28.95	3.428	530	158	2114.42	1.8346	1.6173E-04	1.1945E-04	1.8345E+00	.4522
-4.73	6.3711	0.0000	33.700	1.571	25.00	4.013	530	126	2203.66	2.3136	0.	0.	2.3136E+00	.5737
-3.26	6.3711	.0040	31.950	1.592	28.84	3.901	530	121	2194.45	2.2262	6.9042E-04	4.2027E-04	2.2253E+00	.8495
-1.71	6.3711	.0315	27.730	1.630	28.15	3.585	529	148	2170.88	1.9447	3.2325E-03	2.2526E-03	1.9443E+00	.5619
-.27	6.3711	.1010	20.830	1.680	26.27	3.044	528	185	2131.01	1.4720	6.4153E-03	7.7500E-03	1.4608E+00	.2639
1.40	6.3711	.1402	17.830	1.710	25.22	2.780	527	207	2101.48	1.2675	1.0486E-02	1.1208E-02	1.2536E+00	.1803
3.10	6.3711	.1188	15.400	1.727	25.75	2.891	528	198	2110.15	1.3786	9.4488E-03	5.2878E-03	1.3658E+00	.2155
4.50	6.3711	.0554	24.350	1.727	27.50	3.322	529	165	2146.20	1.7855	5.3649E-03	4.0618E-03	1.7827E+00	.4090
6.12	6.3711	.0086	31.600	1.705	28.77	3.742	530	140	2173.71	2.2183	9.8589E-04	6.0228E-04	2.2165E+00	.7332



(a) Flat-plate detail. Dimensions are in cm.



Injectors at 18.6 cm



Injectors at 24.0 cm

Test	ℓ	a	b	c	D	C_D
1	24.0	0.635	0.578	1.41	0.254	0.830
2	24.0	.152	.680	1.41	.0508	.754
3	24.0	.305	.654	1.41	.1016	.784
4 (ref. 9)	18.6	.3175	.397	.1524	.1016	.760
5 (ref. 12)	24.0	.369	.510	1.41	.123	.830

(b) Injector detail. Dimensions are in cm.

Figure 1.- Experimental model.

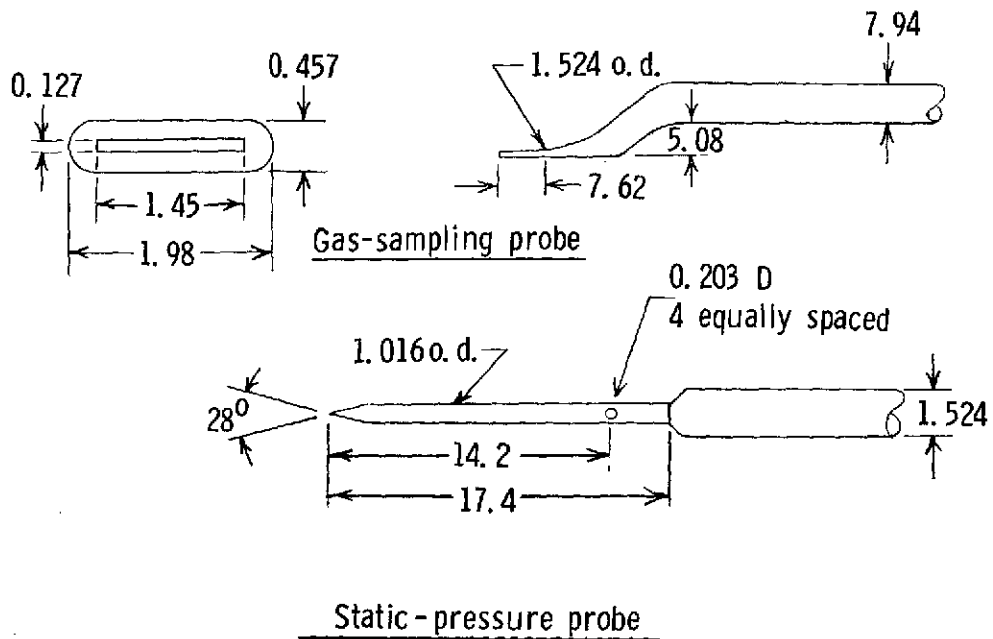


Figure 2.- Survey-probe design. Dimensions are in mm.

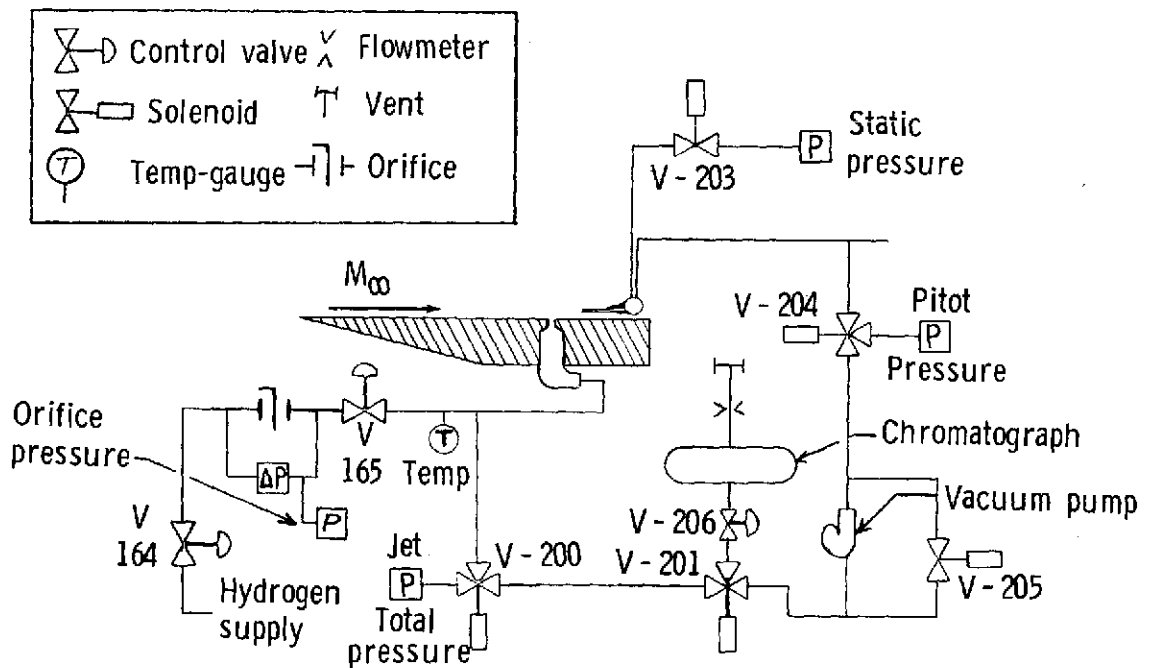


Figure 3.- Schematic of gas sampling system.

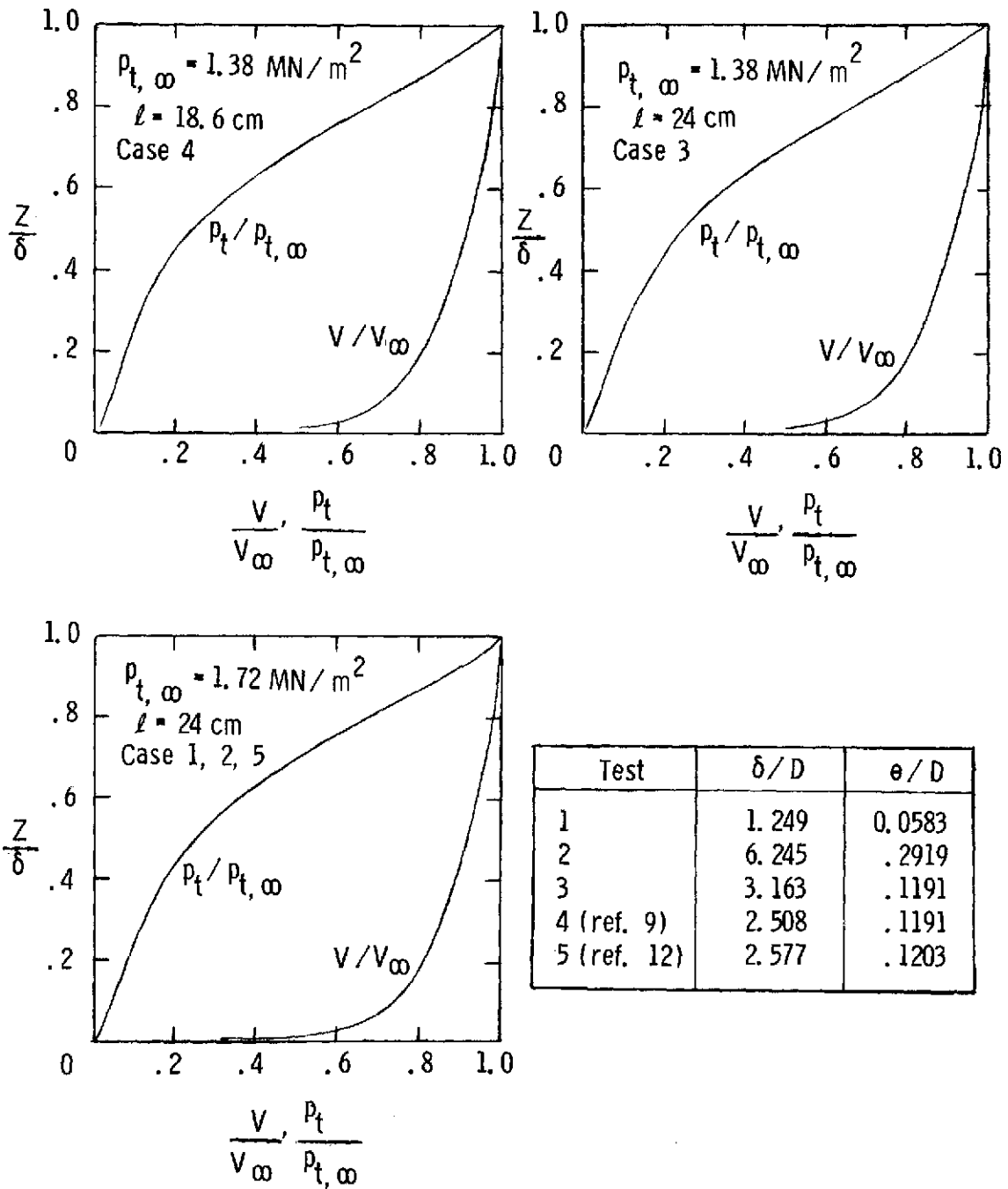


Figure 4.- Undisturbed theoretical plate boundary layer at injector station.

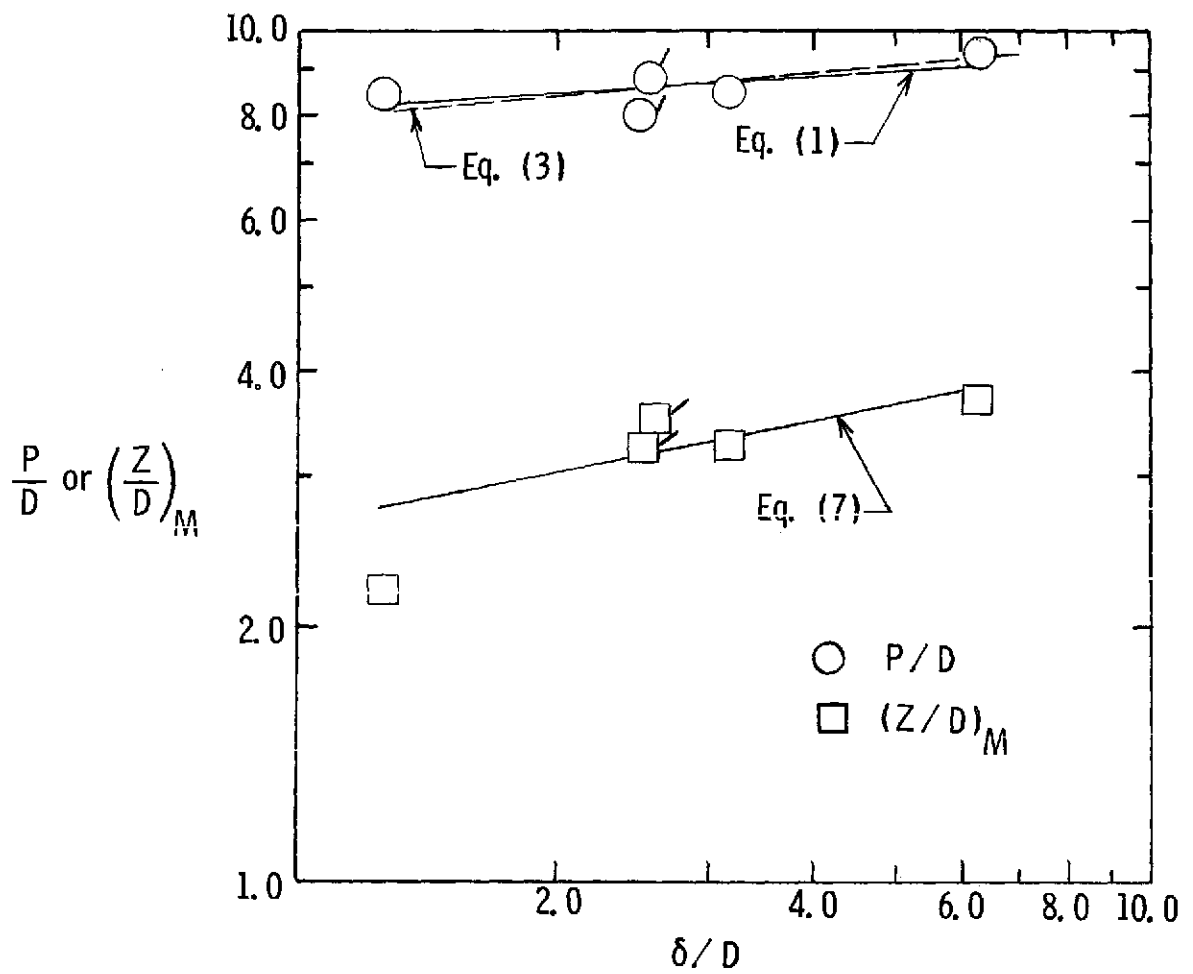


Figure 5.- Jet penetration.

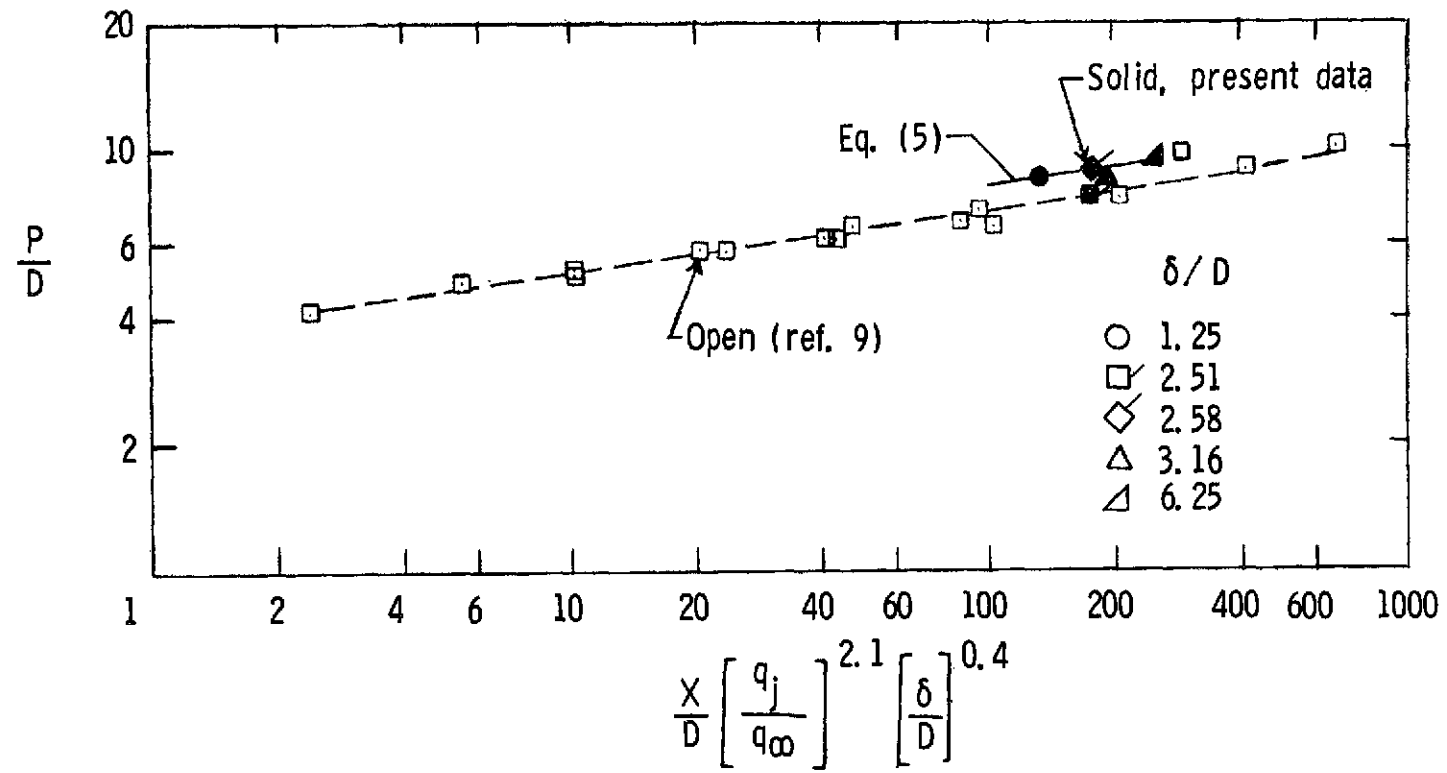


Figure 6.- Correlation of jet penetration.

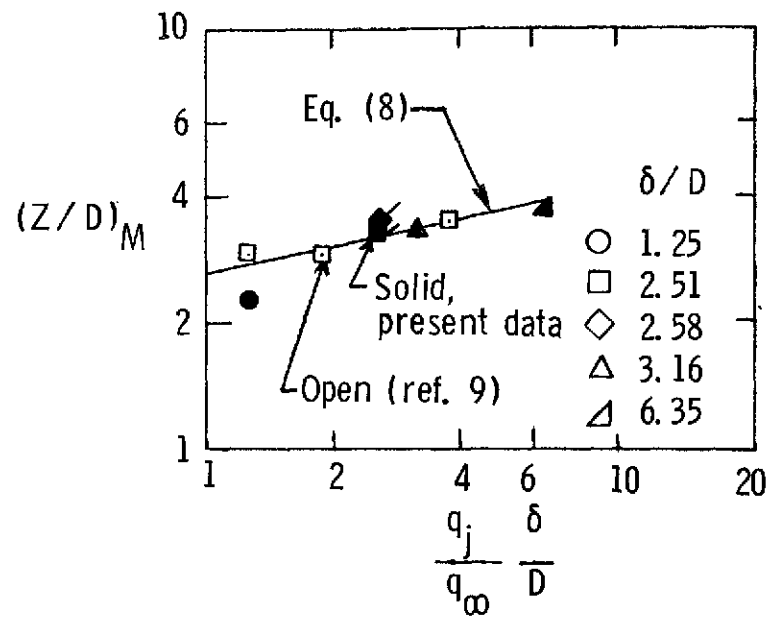


Figure 7.- Correlation of penetration of maximum concentration. $\frac{X}{D} = 120$.

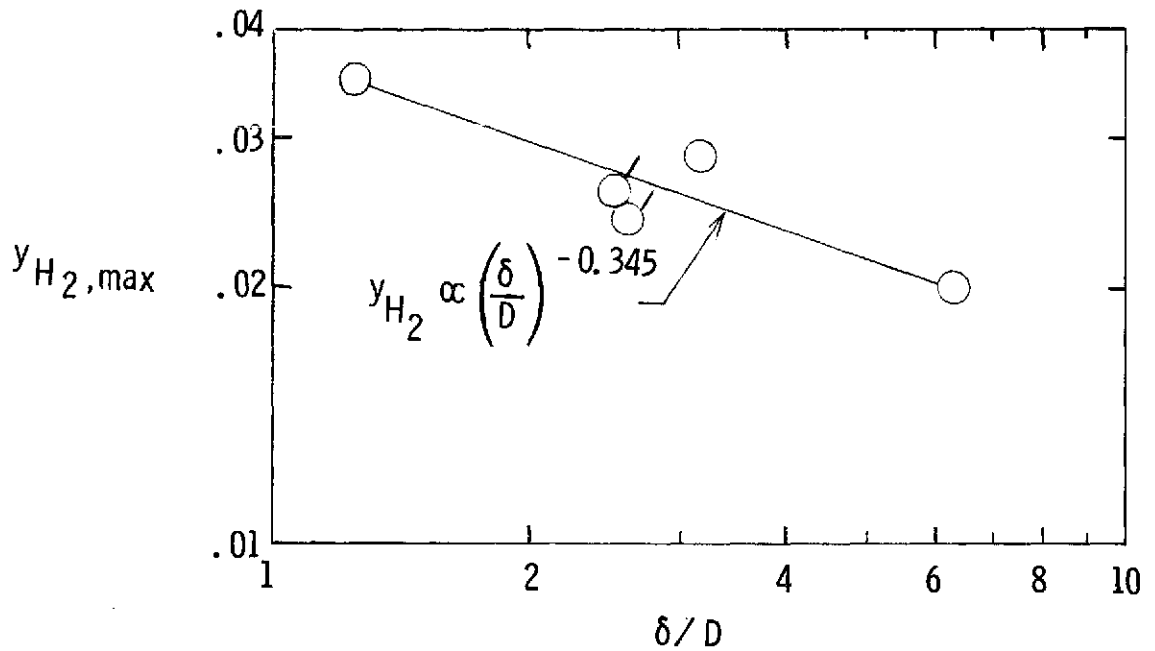


Figure 8.- Maximum hydrogen mass fraction.

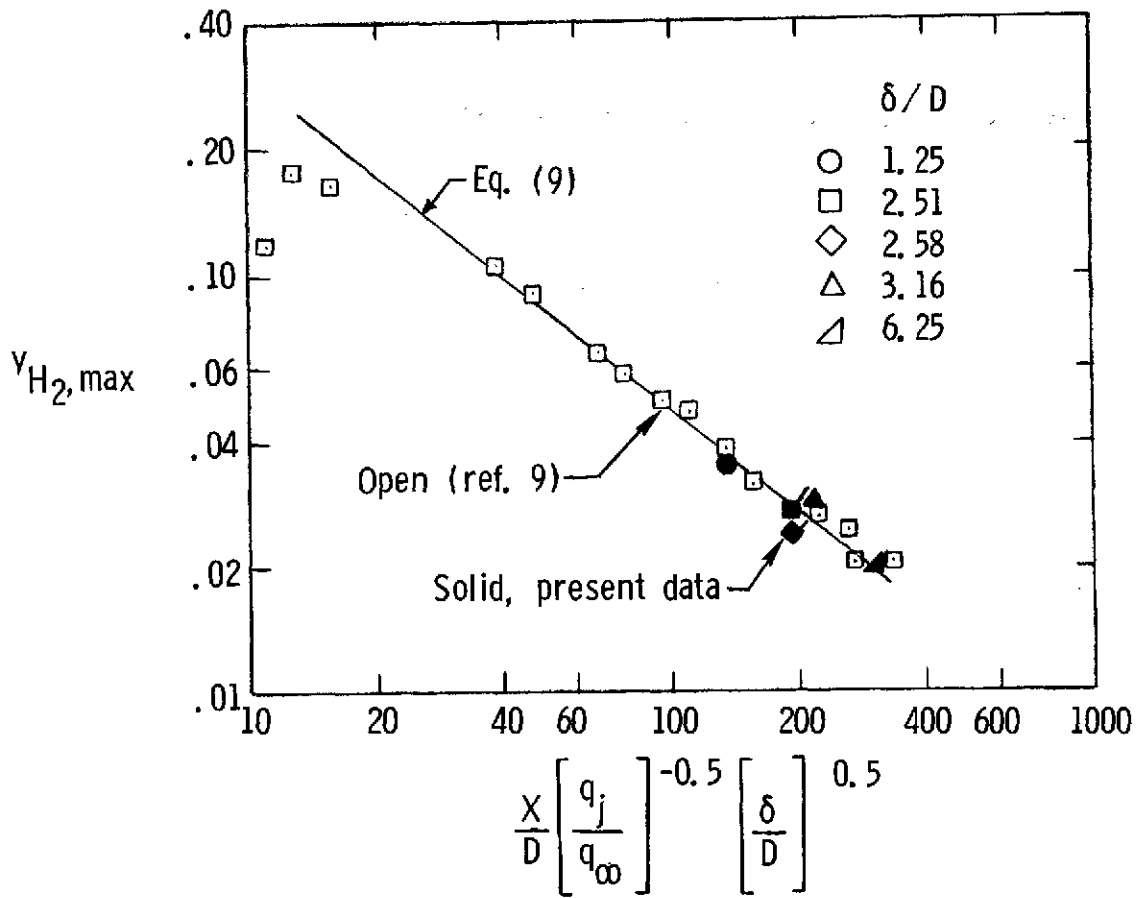


Figure 9.- Correlation of maximum concentration decay.

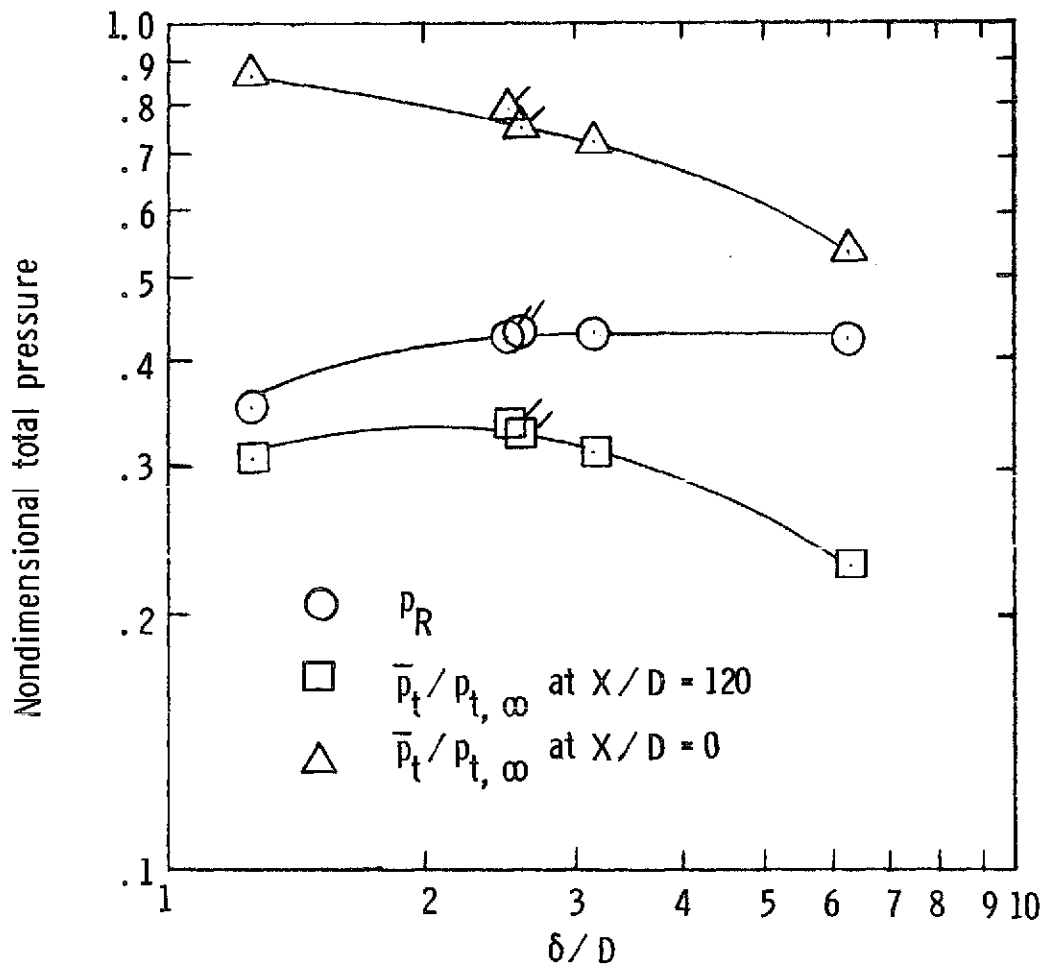


Figure 10.- Mass average total pressure and total-pressure recovery.

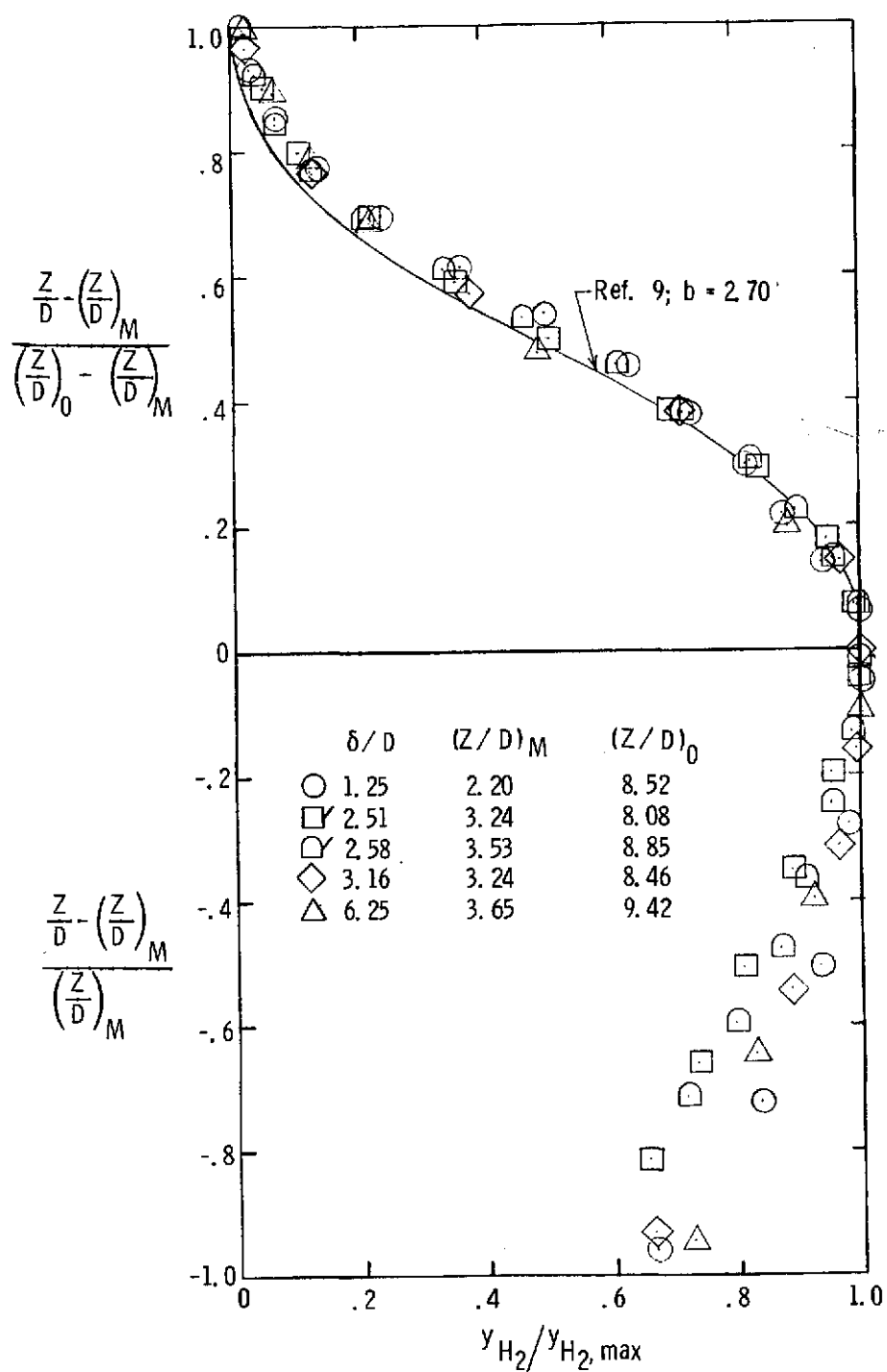


Figure 11. Vertical hydrogen concentration profile.

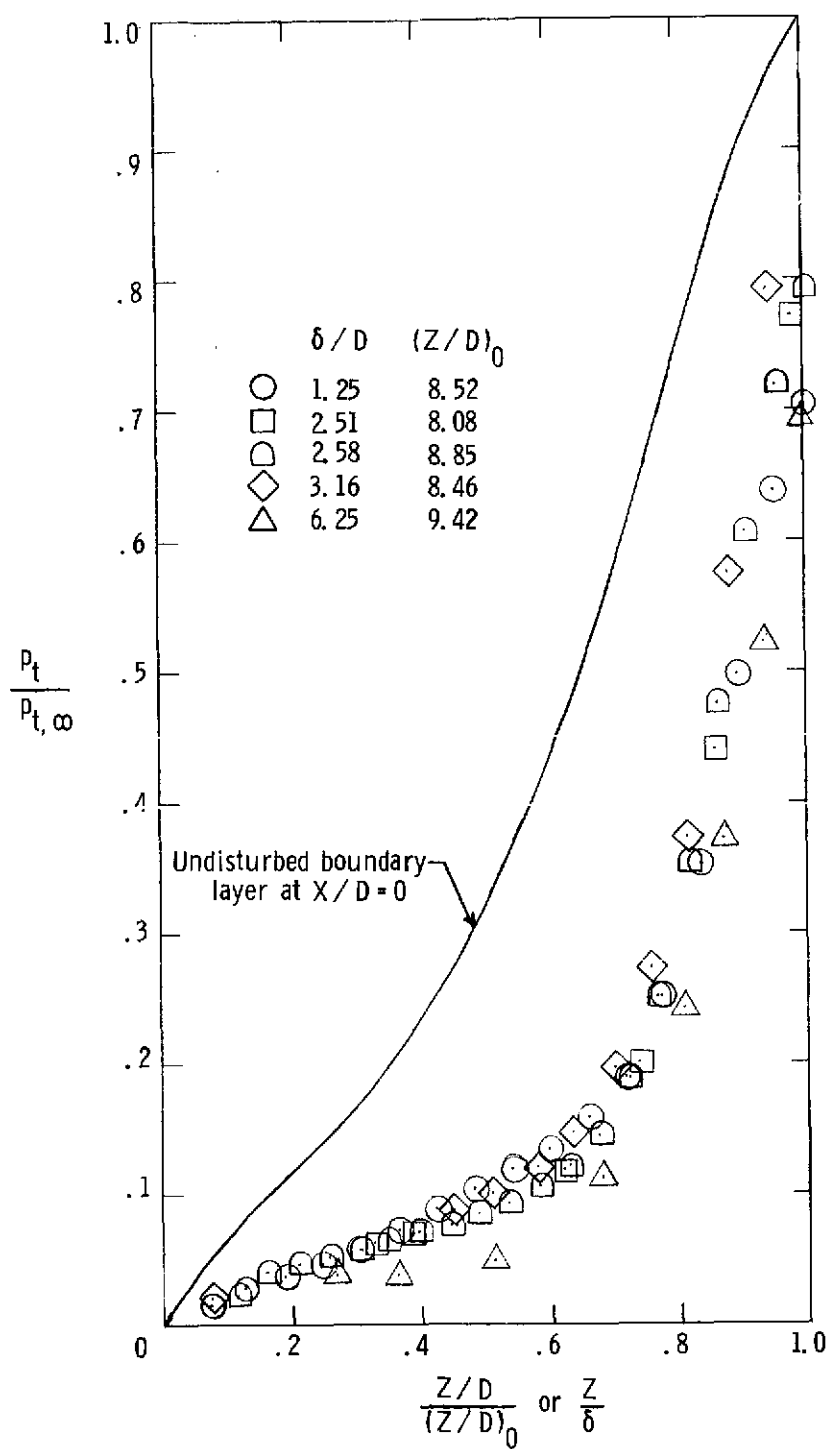
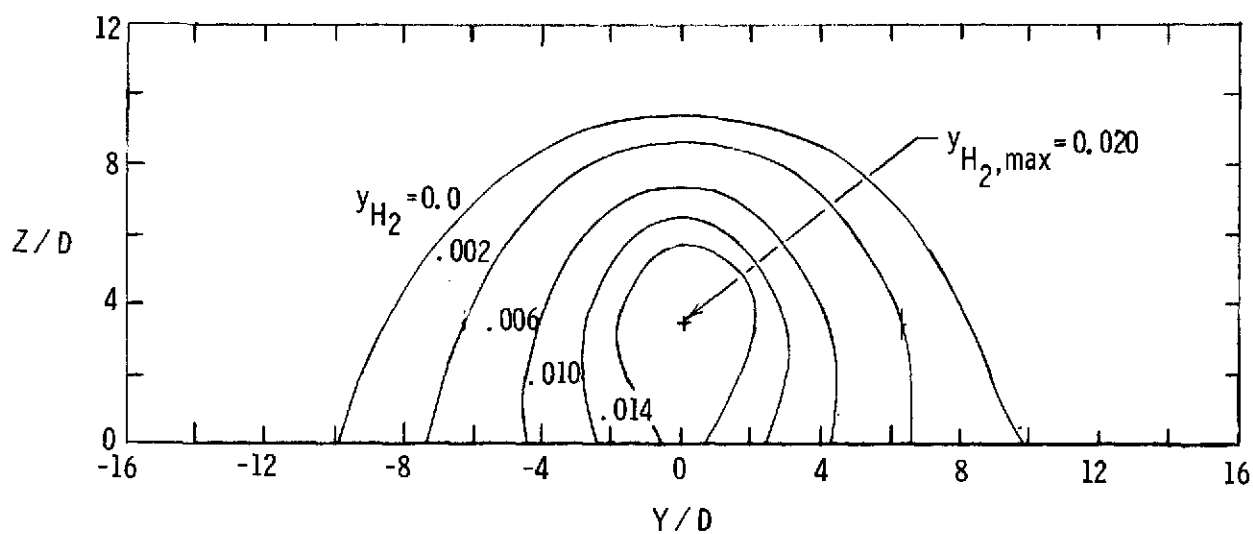
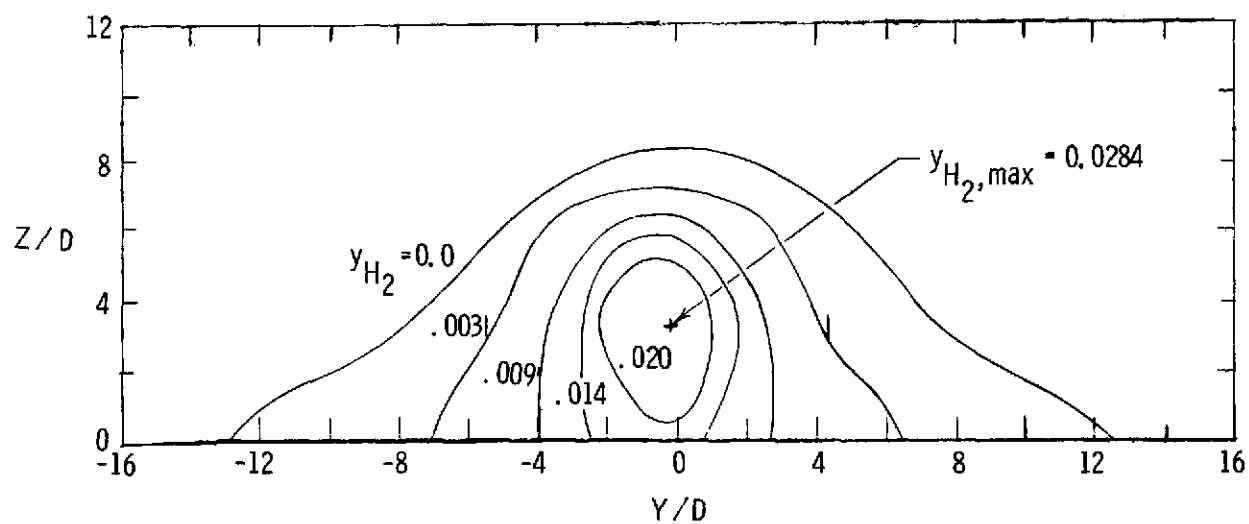


Figure 12.- Vertical total-pressure profile.

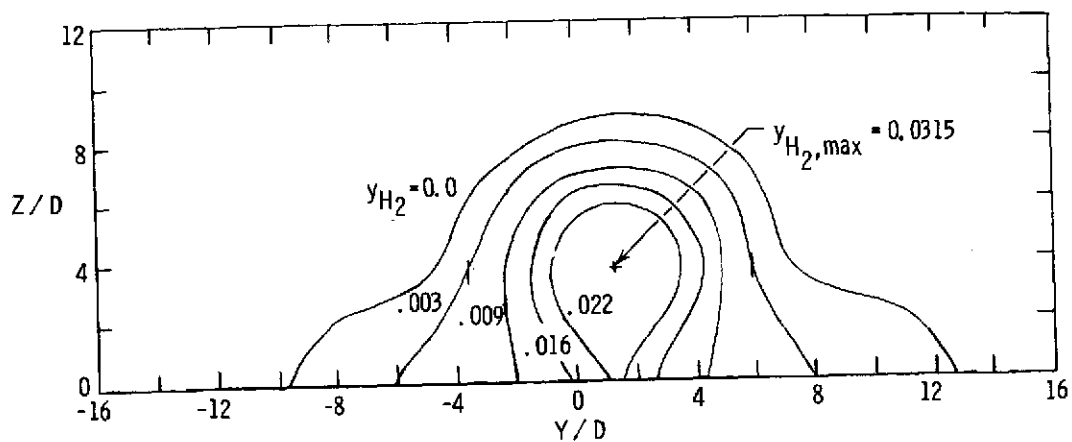


(a) $\frac{\delta}{D} = 6.245$.

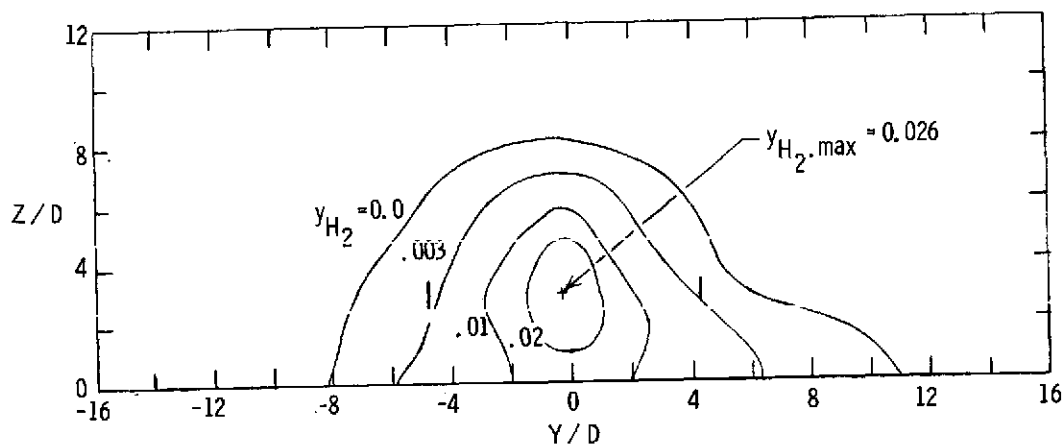


(b) $\frac{\delta}{D} = 3.163$.

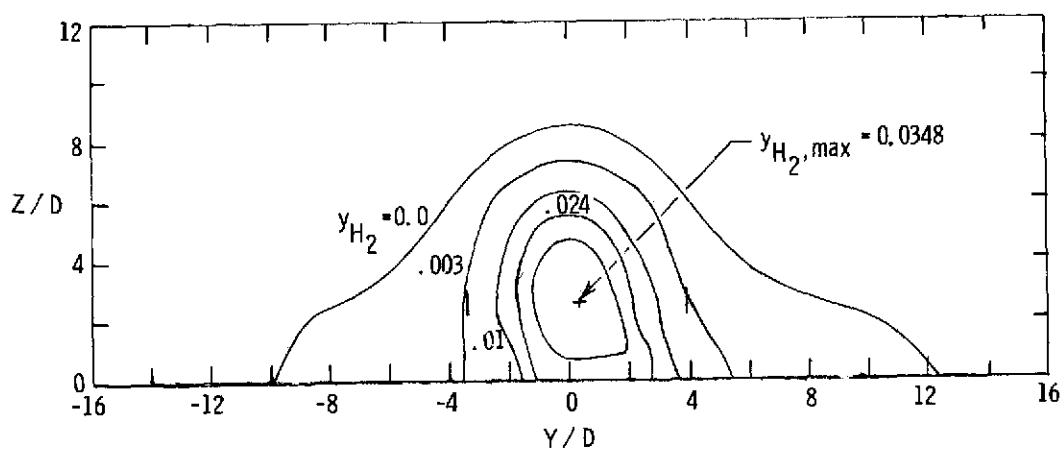
Figure 13.- Hydrogen concentration contour.



(c) $\frac{\delta}{D} = 2.577$.

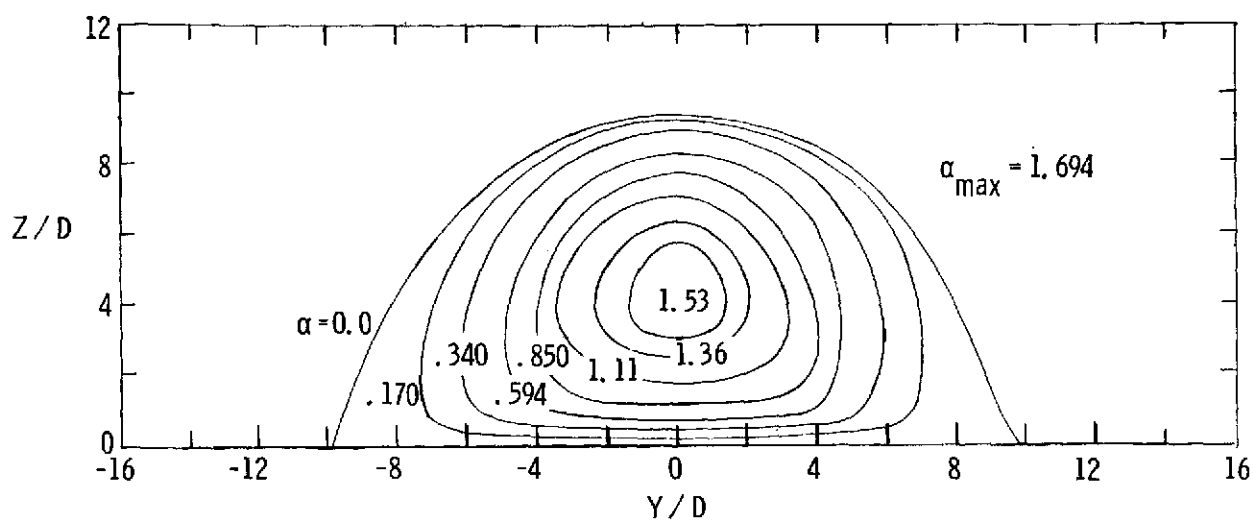


(d) $\frac{\delta}{D} = 2.508$.

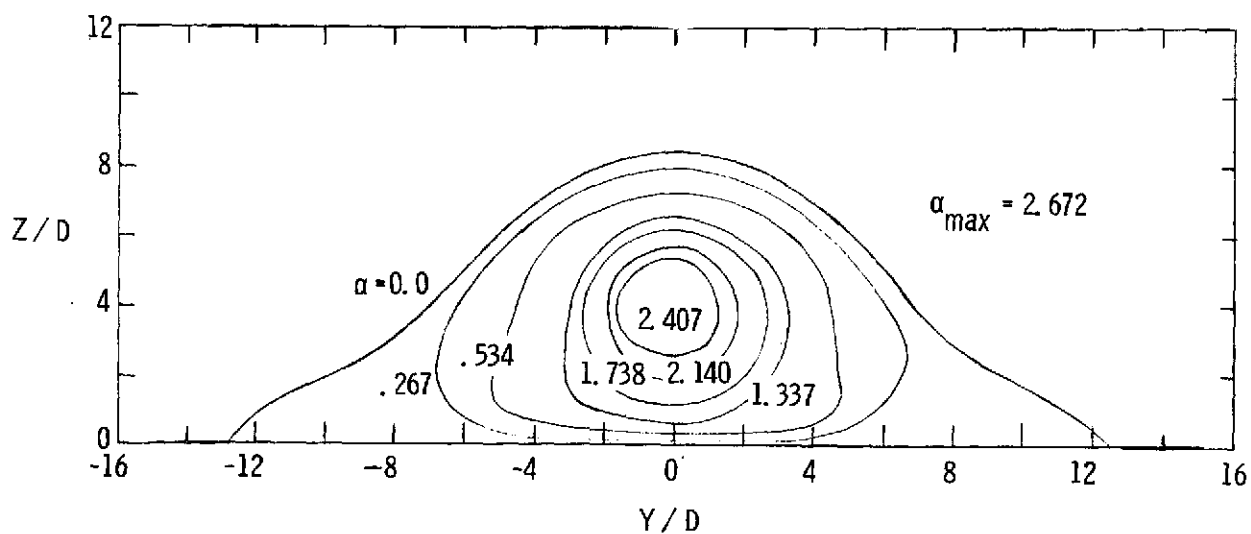


(e) $\frac{\delta}{D} = 1.249$.

Figure 13.- Concluded.

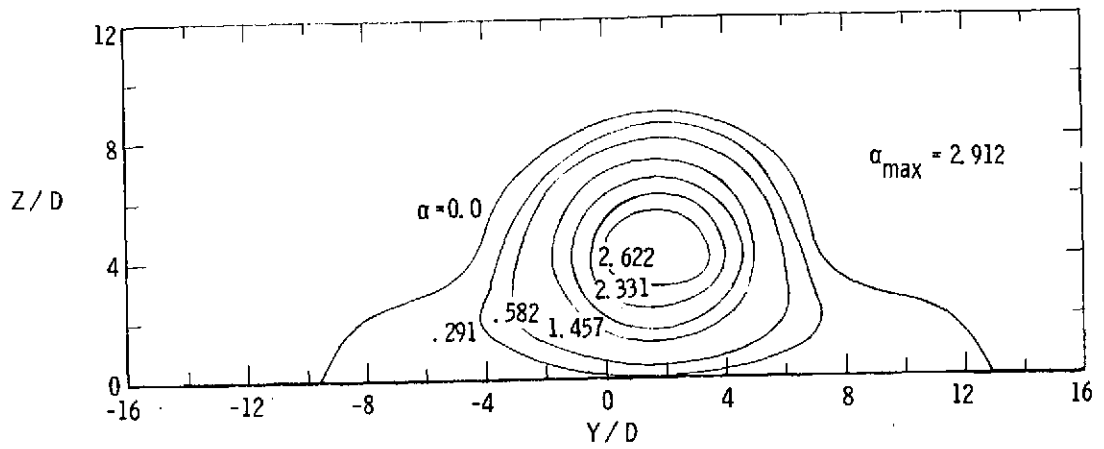


(a) $\frac{\delta}{D} = 6.245$.

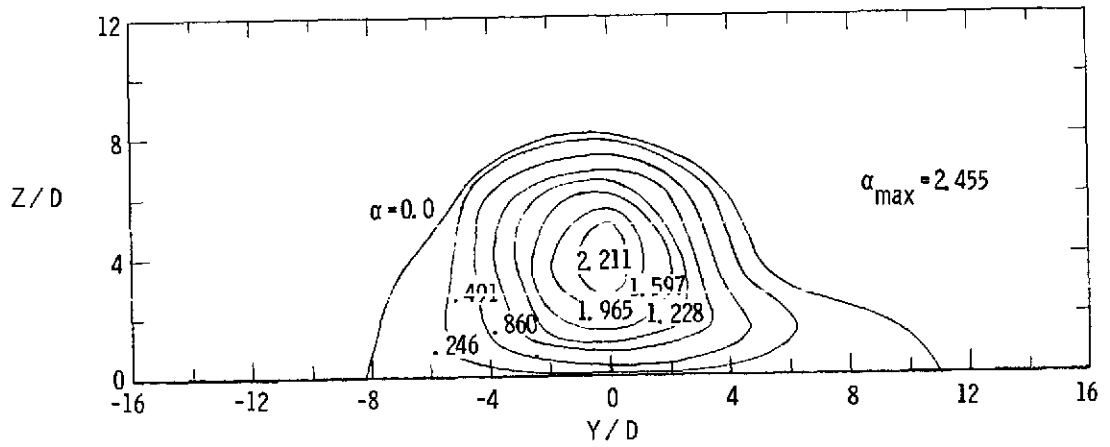


(b) $\frac{\delta}{D} = 3.163$.

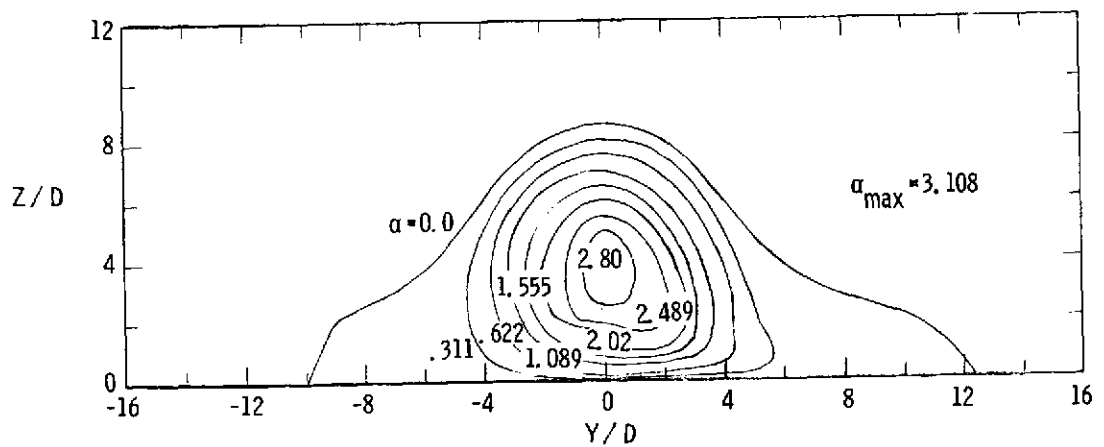
Figure 14.- Hydrogen flow rate contours in $\text{kg/m}^2\text{-sec.}$



(c) $\frac{\delta}{D} = 2.577$.

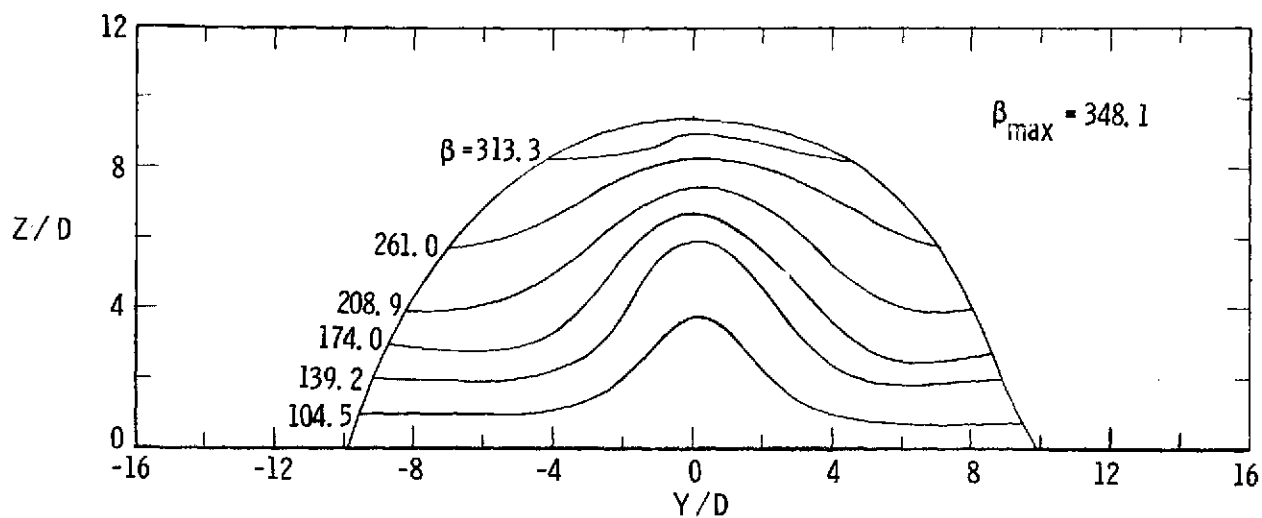


(d) $\frac{\delta}{D} = 2.508$.

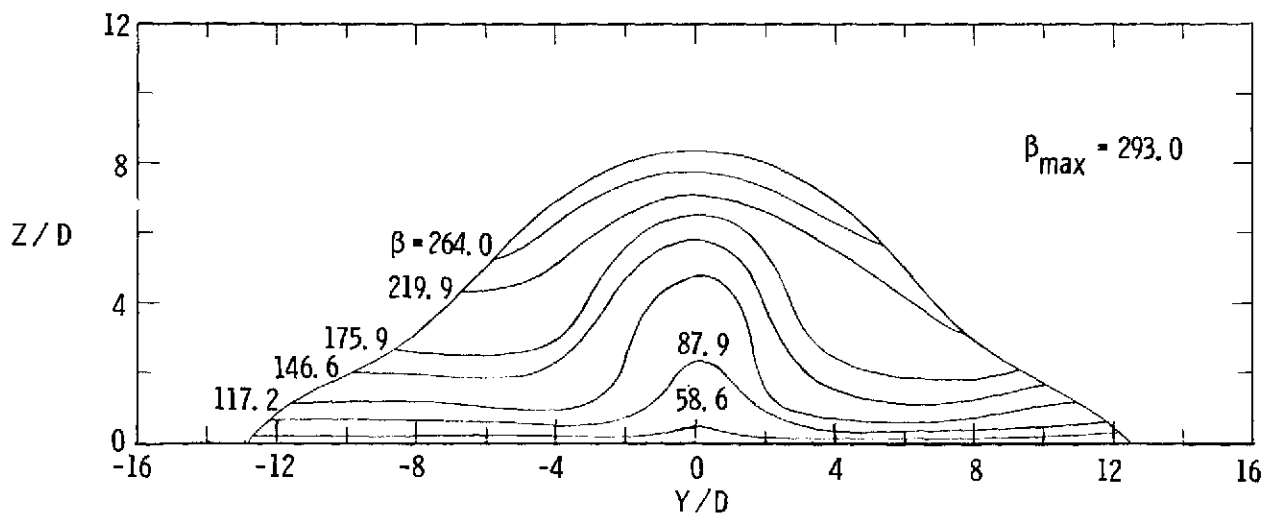


(e) $\frac{\delta}{D} = 1.249$.

Figure 14.- Concluded.

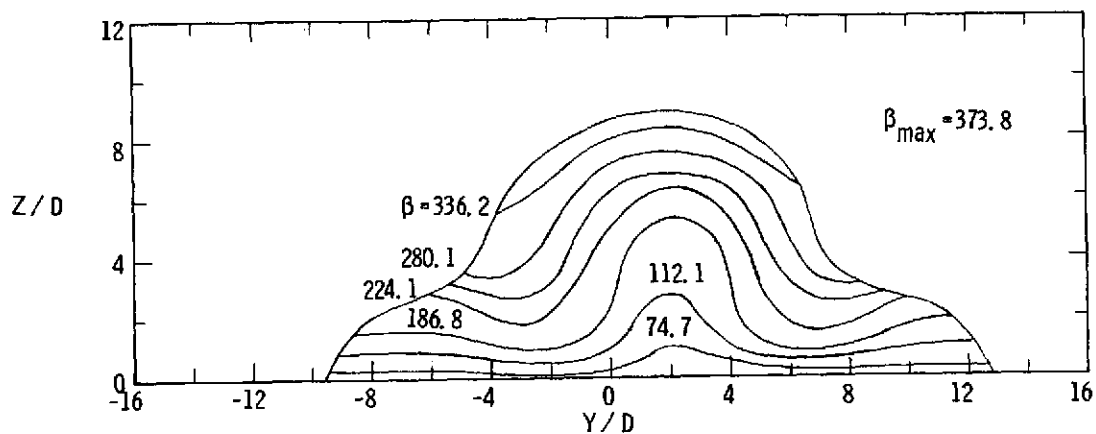


(a) $\frac{\delta}{D} = 6.245$.

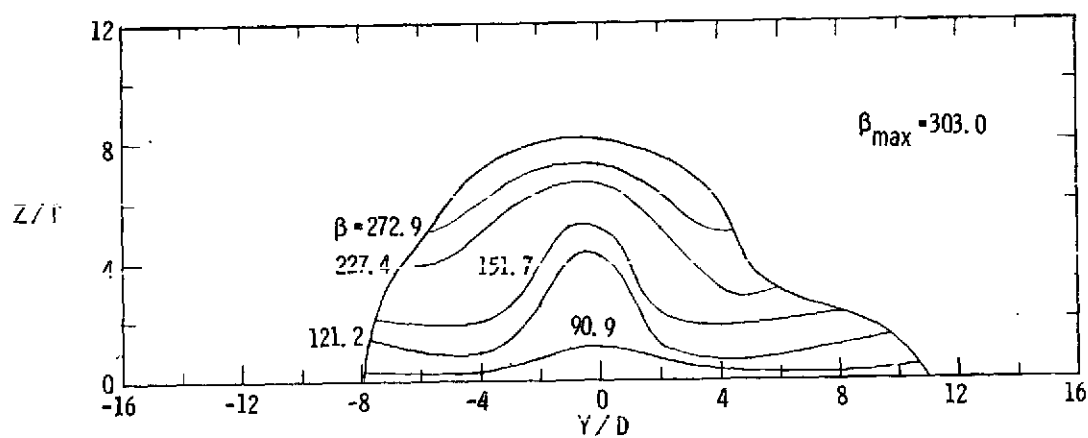


(b) $\frac{\delta}{D} = 3.163$.

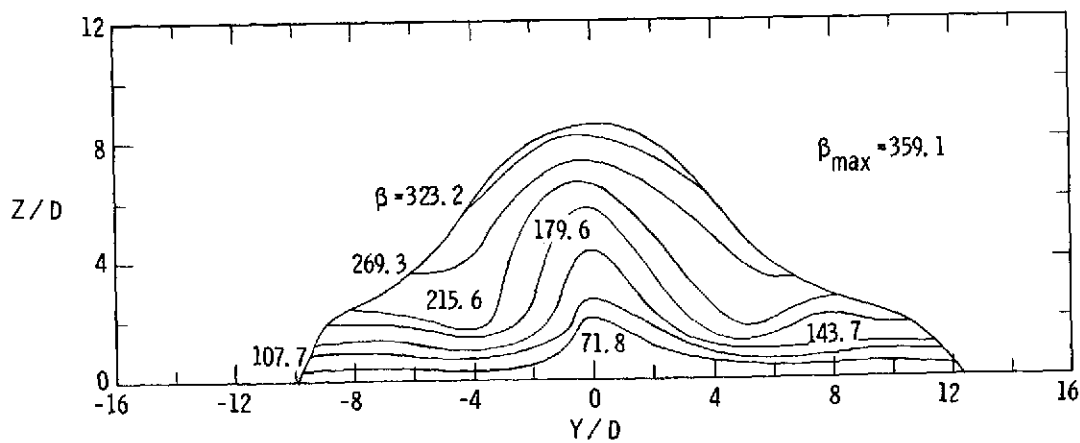
Figure 15.- Airflow rate contours in $\text{kg/m}^2\text{-sec}$.



(c) $\frac{\delta}{D} = 2.577.$

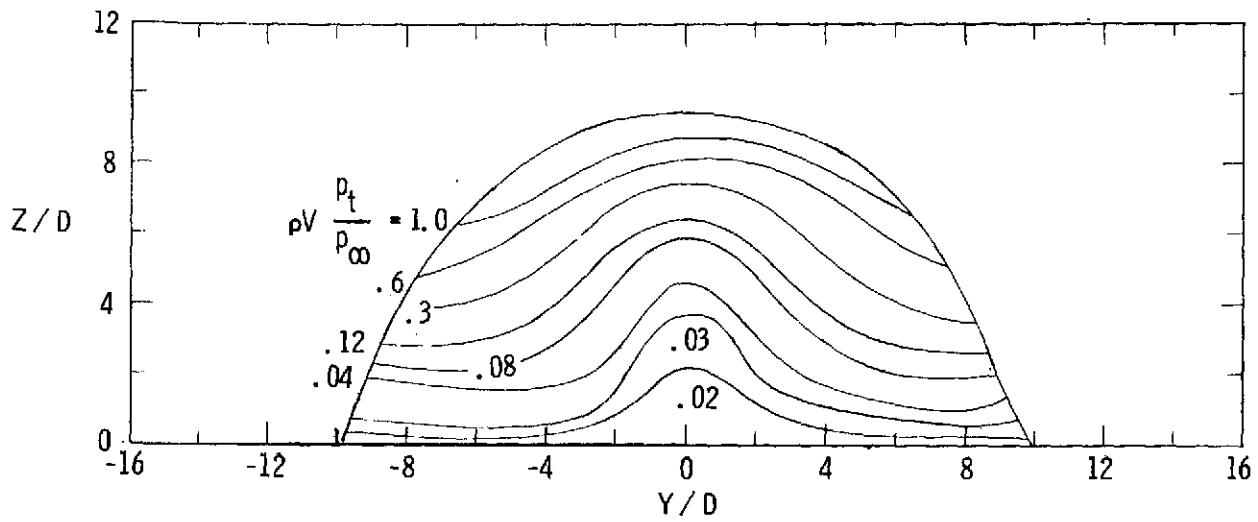


(d) $\frac{\delta}{D} = 2.508.$

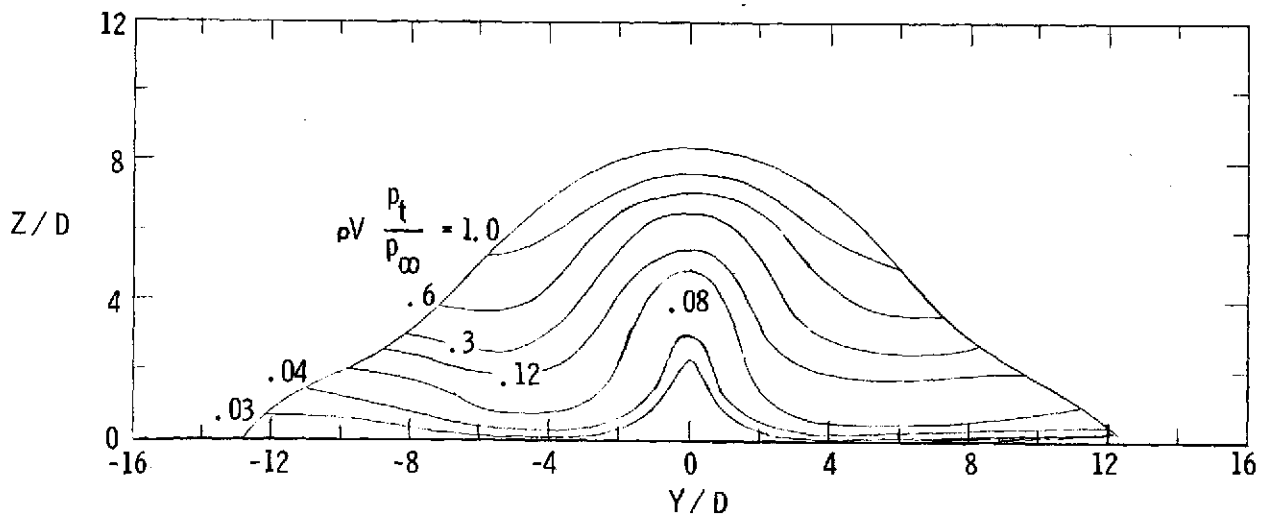


(e) $\frac{\delta}{D} = 1.249.$

Figure 15.- Concluded.

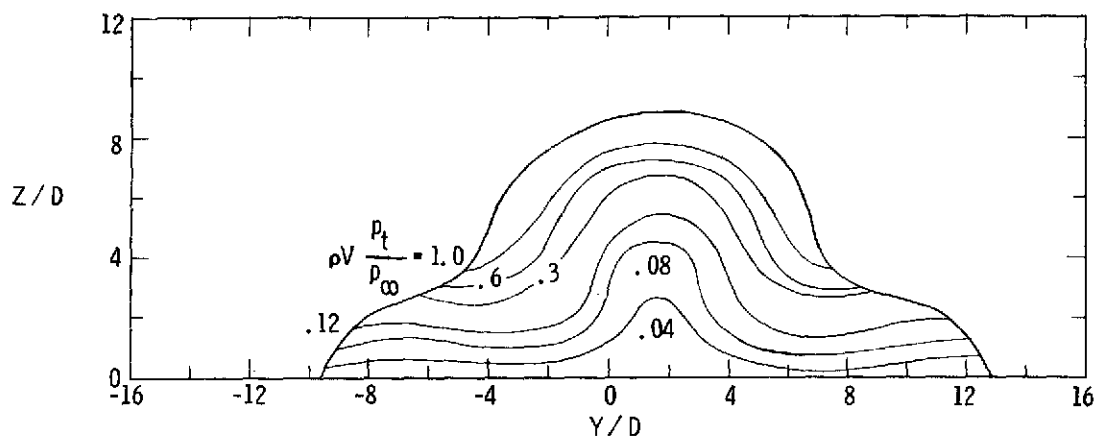


(a) $\frac{\delta}{D} = 6.245$.

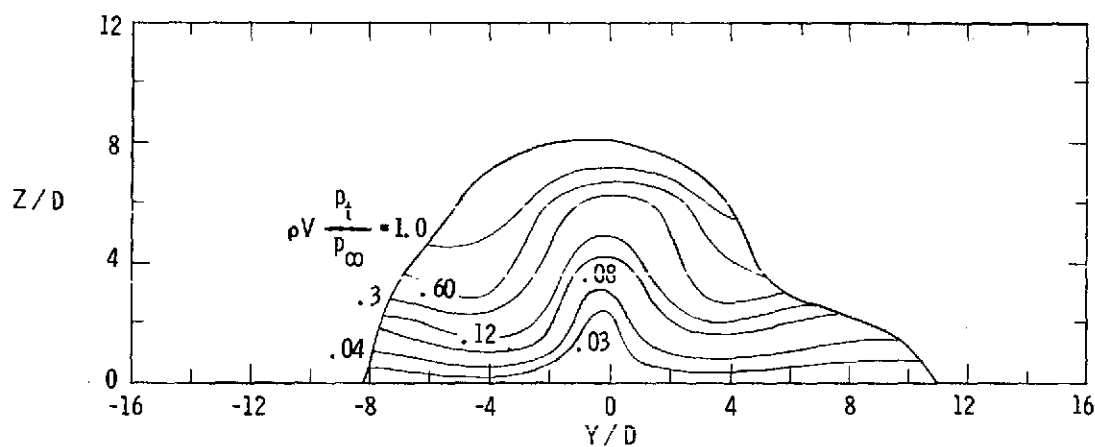


(b) $\frac{\delta}{D} = 3.163$.

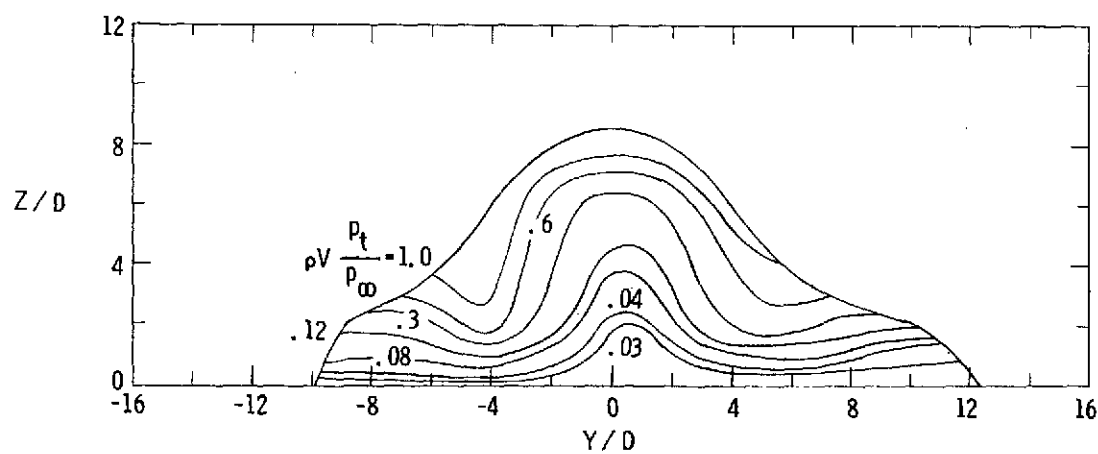
Figure 16. Mass-weighted total-pressure profiles in $\text{kg/m}^2\text{-sec}$.



(c) $\frac{\delta}{D} = 2.577$.



(d) $\frac{\delta}{D} = 2.508$.



(e) $\frac{\delta}{D} = 1.249$.

Figure 16.- Concluded.